NASA TECHNICAL NOTE

NASA TN D-5050

MECHANICAL BEHAVIOR OF BORON-EPOXY AND GLASS-EPOXY FILAMENT-WOUND CYLINDERS UNDER VARIOUS LOADS

by Harvey W. Herring, Robert M. Baucom, and Richard A. Pride

Langley Research Center
Langley Station, Hampton, Va.

NATIONAL AERONAUTICS AND SPACE ADMINISTRATION • WASHINGTON, D. C. • MARCH 1969

NASA TN D-5050

MECHANICAL BEHAVIOR OF BORON-EPOXY AND GLASS-EPOXY FILAMENT-WOUND CYLINDERS UNDER VARIOUS LOADS

By Harvey W. Herring, Robert M. Baucom,
and Richard A. Pride

Langley Research Center
Langley Station, Hampton, Va.

NATIONAL AERONAUTICS AND SPACE ADMINISTRATION

For sale by the Clearinghouse for Federal Scientific and Technical Information
Springfield, Virginia 22151 – CFSTI price $3.00

MECHANICAL BEHAVIOR OF BORON-EPOXY AND GLASS-EPOXY FILAMENT-WOUND CYLINDERS UNDER VARIOUS LOADS

By Harvey W. Herring, Robert M. Baucom,
and Richard A. Pride
Langley Research Center

SUMMARY

A study was made to determine the mechanical behavior of boron-epoxy and S-glass—epoxy filament-wound cylinders under tensile, compressive, torsional, and pressure loads. These cylinders were fabricated in either an orthotropic winding pattern or an isotropic pattern. Conventional theory used to predict the elastic behavior of glass-epoxy filament-wound cylinders was discovered to be equally adequate for the boron-epoxy cylinders. Since Young's modulus for a boron filament is much greater than that for a glass filament, the boron-epoxy cylinders were considerably stiffer than those of glass-epoxy. Attempts to correlate cylinder failure strengths calculated from existing state-of-the-art theories with experimental failure strengths met with varying success. Thus, additional research is necessary before failure characteristics of filament-wound composite cylinders, either glass- or boron-reinforced can be accurately predicted.

INTRODUCTION

The utility of conventional composite materials made by imbedding fibrous glass in a suitable resinous matrix is universally recognized. Glass-reinforced epoxy or polyester materials, which are strong, lightweight, inexpensive, and easily fabricated, are used in many commercial and military structural applications. However, one inherent, often undesirable, characteristic of glass-reinforced composites is their low stiffness. Values of Young's modulus determined from tests of these materials typically range from 2×10^3 to 8×10^3 ksi (14 to 55 GN/m^2); these values depend on the winding pattern of the composite and on the volume fraction of filament in the composite.

Boron filaments with about half the tensile strength, nearly equal density, and 5 to 6 times the stiffness of glass filaments have recently been developed. Boron-reinforced composites may therefore be more applicable than glass-reinforced composites to structures where stiffness is a primary design consideration.

As a result, a research program was initiated at the NASA Langley Research Center to explore the potential of boron filament as a composite-material reinforcement

for possible use in aerospace vehicle structures. This research has been conducted in three separate phases. First, the investigation was concerned with a comprehensive survey of commercially available boron monofilament. A comparison of selected mechanical and physical properties of 12 different boron filaments is presented in references 1 and 2. The second phase of the investigation involved designing and testing uniaxial boron-filament-reinforced-epoxy composites in the form of simple rings and belts. This work is described in reference 3.

The third phase of the research program, reported herein, was concerned with the design, fabrication, and testing of multilayered, multidirectional filament-reinforced-epoxy circular cylinders. Seven boron-epoxy and six S-glass—epoxy bottles were fabricated. Orthotropic and isotropic reinforcement winding patterns were used in the fabrication. A cylinder cut from each bottle was subjected to either axial compression, tension, torsion, internal pressurization or external pressurization so that elastic constants could be determined for each loading condition, and failure strengths were determined for three loading conditions. In the present paper the structural behavior of the boron-epoxy cylinders is compared with that of the glass-epoxy cylinders, and experimentally derived elastic constants and failure strengths are compared with values calculated from existing theory.

SYMBOLS

The units used for the physical quantities defined in this paper are given both in U.S. Customary Units and in the International System of Units (SI) (ref. 4). Appendix A presents factors relating these two systems of units.

E	Young's modulus
G_{xy}	shearing modulus of cylinder wall
P	axial load
p	pressure
r	cylinder radius
S	allowable shearing strength of unidirectional layer associated with directions parallel and perpendicular to filaments
t	wall thickness of cylinder

V	volume fraction of constituent in composite cylinder
X,Y	allowable strengths of unidirectional layer in directions parallel and perpendicular to filaments, respectively
ϵ	strain
μ_{xy}	Poisson's ratio associated with strain in circumferential direction induced by load applied in longitudinal direction
μ_{yx}	Poisson's ratio associated with strain in longitudinal direction induced by load applied in circumferential direction
σ	normal stress
τ_{LT}	shear stress in a layer associated with directions parallel and perpendicular to the filament

Subscripts:

c,t	measured under compressive and tensile loads, respectively
f	filament
L,T	directions parallel and perpendicular to filaments in a unidirectional layer, respectively
r	resin
v	void
x,y	longitudinal and circumferential directions, respectively

TEST SPECIMENS

Fabrication

Seven boron-epoxy and six glass-epoxy filament-wound bottles were fabricated, each with a 3-inch (7.6-cm) inside diameter and approximately 9 inches (23 cm) long. The two filament winding patterns that were used in this investigation are shown

schematically in figure 1. The orthotropic pattern, consisting nominally of a 2-to-1 ratio of circumferential to longitudinal windings, was used in four boron-epoxy and three glass-epoxy bottles and was considered to be an optimum filament arrangement for internal pressure loading. The orthotropic winding sequence was two circumferential – two longitudinal – two circumferential for a total of six layers. The remaining six bottles, three boron-epoxy and three glass-epoxy, were wound in an isotropic pattern, a series of alternating layers of circumferential and opposed helical wraps nominally at 30° to the longitudinal axis of the cylinder. The isotropic winding sequence was two opposed helical – one circumferential – two opposed helical – one circumferential for a total of six layers. The isotropic pattern was chosen for study because it provided a better balance of elastic behavior for bending, compression loads, or torsion loads (ref. 5).

Each of the four bottle types is shown in figure 2. The difference between the end dome configurations of the isotropic and orthotropic bottles was necessitated by the different wrapping angles. Both the orthotropic and the isotropic winding patterns deviated from the nominal configuration. In the orthotropic pattern, the longitudinal filaments were wrapped at a 7° angle to the longitudinal axis to clear the mandrel end bosses. (See fig. 3.) The helical filaments in the isotropic pattern were wrapped at a 33° instead of a 30° angle to the longitudinal axis because of an error in setting up the winding machinery. Boron-epoxy tape is shown being wound onto a salt mandrel in the longitudinal mode in figure 3, in the circumferential mode in figure 4, and in the helical mode in figure 5.

For the glass-epoxy isotropic bottles, winding densities were 263 ends/inch (104 ends/cm) for each helical layer and 247 ends/inch (97 ends/cm) for each circumferential layer. For the boron-epoxy isotropic bottles, these densities were 1320 filaments/inch (520 filaments/cm) for each helical layer and 1235 filaments/inch (486 filaments/cm) for each circumferential layer. Winding densities for the glass-epoxy orthotropic bottles were 333 ends/inch (131 ends/cm) for each longitudinal layer and 333 ends/inch (131 ends/cm) for each circumferential layer. For the boron-epoxy orthotropic bottles, these densities were 1665 filaments/inch (655 filaments/cm) for each longitudinal layer and 1667 filaments/inch (656 filaments/cm) for each circumferential layer.

The bottles were fabricated by winding continuous boron or glass filament preimpregnated with epoxy resin onto the surface of a salt mandrel with the desired shape of the finished bottle. Heat guns were used as shown in figure 4 to soften the resin in the preimpregnated tape and insure its uniform coverage of the wound surface. Consolidation of filaments and epoxy matrix occurred when the resin was subjected to an elevated-temperature curing treatment (2 hours at 200° F (360° K) followed by 2 hours at 300° F (420° K)). The mandrels (figs. 3, 4, and 5) were cast from a low-melting water-soluble salt, which was subsequently washed out of the cured bottle.

Materials

The resin system selected was the EPON Resin 826 used with the Z curing agent. This epoxy resin system was chosen because it is relatively easy to apply in a filament-winding operation and has good mechanical and physical properties after a moderate curing treatment. The stress-strain behavior of this resin system in both tension and compression is shown in figure 6.

A 1.7-mil (43-μm) diameter halide-process boron filament (filament A of ref. 1) which was incorporated into a 20-strand preimpregnated tape, was used in this study. The glass filament was supplied in the form of a commercially available 20-end S-glass roving that had been preimpregnated with the epoxy resin. Typical tensile properties and densities of the materials used in this investigation are listed in table I.

Specimen Configuration

Right circular cylinders 6 inches (15 cm) long cut from each bottle were used as test specimens to facilitate the application of different loads on a single specimen. The ends of each cylinder were reinforced by circumferential overwrapping to prevent their delamination during testing. Small cylindrical sections or segments of such sections cut from failed cylinders were used for photomicrography and for the determination of resin and void content. Average wall thicknesses and average wall densities for the cylinders tested are listed in tables II and III, respectively. The cylinders are identified by the failure load to which they were subjected, that is, internal pressure, external pressure, or axial compression. One of each of the four cylinder types was failed under each loading condition except that two orthotropic boron-epoxy cylinders were failed under internal pressurization and yielded duplicate values for this particular test.

TEST PROGRAM

Objectives

The purpose of the test program was to evaluate the performance of boron-epoxy cylinders under a variety of loading conditions and to compare their performance with that exhibited by similar glass-epoxy cylinders and with theoretical predictions based on existing theory. The test program was divided into two parts. The first part was concerned with the elastic response of the cylinders to applied loads, and the second with their failure characteristics.

Elastic Constants

The test program to determine the elastic behavior of the cylinders is summarized in figure 7. The types of loads to which the cylinders were subjected and the elastic

constants determined from each loading condition are shown. Eleven cylinders were loaded longitudinally in tension and compression, loaded circumferentially in torsion, and subjected to internal lateral and external lateral pressure; all loads were within the elastic range of the cylinders. The elastic limits of the cylinders were estimated in advance of the tests from a knowledge of the filament orientation and of the stress-strain characteristics of the filaments and resin. These estimated elastic limits were determined both in terms of a limiting stress and a limiting strain; and to ensure conservative results, a test was terminated when the first limiting value was reached. In this manner, Young's moduli in the longitudinal direction and associated Poisson's ratios were established for both tension and compression by the axial loading tests. These quantities in the circumferential direction were obtained from internal pressure tests for tension and from external pressure tests for compression. Shear moduli were obtained similarly from simple torsion tests. Data were collected in the form of load-strain curves, and elastic constants were determined from the slopes of these curves.

Test Methods

In preparation for testing, wire strain gages were bonded to the surfaces of each cylinder as shown in figure 8. For the axial loading and pressurization tests, two circumferential and three longitudinal gages were spaced as shown along the inner and outer circumferences of each cylinder midway along its length. These inner and outer gages were placed back-to-back to record any bending during a test. For the torsion tests, rosette gages were attached to opposite sides of the exterior of the cylinders to record strains at $\pm 45^{\circ}$ with respect to the cylinder longitudinal axis. Strain was recorded in the Langley central digital data recording facility at a virtually continuous rate.

Axial compression.- An isotropic glass-epoxy cylinder is shown under compression in figure 9. The cylinder is seated on a base plate which has been drilled to allow the interior strain-gage leads to pass through to the outside. The ends of each cylinder were cut flat and parallel to insure good specimen alinement during compression testing.

Axial tension and torsion.- For tension and torsion testing, the ends of each cylinder were potted in the fixtures shown in figure 10. One end of the fixture was machined to accept the cylinder plus a thin epoxy bond on either side of the cylinder wall. On the other end was a square boss which mated to a socket on the torsion testing machine. The fixture was drilled and tapped to accept rods from the tensile testing machine. Cylinder-fixture alinement was achieved by shimming before applying the epoxy bond. Interior strain-gage leads were brought out through holes drilled in the end fixtures. An isotropic glass-epoxy cylinder is shown in tension in figure 11 and in torsion in figure 12.

Internal pressure.- Internal pressure loads were applied hydraulically by a small hand-operated jack and suitable plumbing. A fixture was devised (fig. 13) which provided

an effective hydraulic seal yet imposed negligible end restraint on the cylinder being tested. The absence of end restraint was observed by sliding the cylinder back and forth on the test fixture after pressurization. Two end plugs were machined with "O" ring grooves to provide a tight seal in the cylinder ends. The interior ends of the plugs were drilled and tapped to accept a steel bar that served to keep the plugs from being ejected from the cylinder by the fluid pressure. The fixture was appropriately drilled and fitted to allow for influx of hydraulic fluid, bleeding, and readout of interior strain gages. When seepage leaks due to porosity in the cylinder walls occurred, a liner of either dental dam, chlorobutyl rubber, motorcycle innertube, or aluminum sheet was used, the severity of the leak determining which material. An isotropic glass-epoxy cylinder with the fixture for internal pressure testing inserted is shown in figure 14.

External pressure.- The procedure for external pressure testing was similar to that for internal pressure testing except that the internal-pressure fixture was used as a seal against external pressure and that the interior of the cylinder was vented to the atmosphere. A cylinder with the internal-pressure fixture inserted was placed inside a chamber as shown in figure 15. If a bladder was necessary, it was placed around the exterior of the cylinder. The outer chamber with the test cylinder inside and ready for pressurization is shown in figure 16.

Failure Tests

All 13 cylinders were failed under either axial compression, internal pressurization, or external pressurization. Failures induced by axial tension or by torsion were not obtained because of insufficient bond area between the walls of the cylinders near their ends and the adapting end of the test fixtures. The procedures for loading the cylinders to failure were the same as for the elastic tests except for the magnitude of the load required.

Determination of Filament, Resin, and Void Content

In order to properly assess the structural performance of the composite cylinders, determination of the relative volumes of filament, resin, and void in each specimen is necessary. The average component volume fractions for 12 cylinders are listed in table IV.

Boron composites.- The method used for the determination of filament, resin, and void content in a sample of boron-epoxy composite material involved combustion of the composite sample in such a manner as to convert all the carbon in the sample to carbon dioxide gas (CO_2). Combustion was achieved in a standard machine used in the metallurgical industry to determine carbon content of alloys and coke fuel. By comparing the quantity of CO_2 thus produced with that obtained from combustion of a resin blank,

the weight fraction of resin in the original sample could be calculated. By knowing the weight and volume of the original specimen and the densities of resin and boron filaments, the respective volume fractions of filament, resin, and void were calculated.

Glass composites.- Since glass does not oxidize at moderately elevated temperatures, determination of filament, resin, and void content in glass-reinforced composites was easily accomplished by burning the resin out of a composite sample at 1000° F (811° K). When a constant residual weight was recorded, only glass remained. By appropriate weighing and measuring, volume fractions of glass filament, resin, and void were calculated.

Composite Photomicrography

Both transverse and longitudinal sections were cut from each cylinder and prepared for photomicrographic examination. The transverse sections were those cut perpendicular to the longitudinal axis of the cylinder, and the longitudinal sections were those cut parallel to that axis. These specimens were mounted in bakelite and then were given a vibratory polishing for 4 hours on nylon cloth laden with microscopic alumina particles in preparation for observation.

Boron-epoxy cylinder sections.- Both transverse and longitudinal sections cut from the wall of an orthotropic boron-epoxy cylinder are shown in figure 17. The entire cylinder wall thickness is shown, and the wrapping sequence is circumferential – longitudinal – circumferential. The black areas around most of the filaments do not necessarily represent voids in the specimens. The boron filaments are so hard that during polishing the resin surrounding each filament is worn away to a depth which is out of focus at the magnification of the figure; thus, black areas around most of the filaments are shown. If the resin continues to be worn away, however, the unsupported filament end may break off. This occurrence may be responsible for some of the gross voids indicated in figure 17.

Glass-epoxy cylinder sections.- In figure 18 typical tranverse and longitudinal sections from an orthotropic glass-epoxy cylinder are shown. Again the entire cylinder wall thickness is shown with circumferential wraps at the inner and outer surfaces and the longitudinal reinforcement in the center. Voids, filaments, and resin pockets are indicated on the figure. In the longitudinal section separations, or delaminations, occur between the layers and within the longitudinal layer. These delaminations cause the longitudinal section to be thicker than the transverse section. These specimens were taken from cylinders which had been loaded to failure, and the delaminations probably resulted from the applied load.

RESULTS AND DISCUSSION

Elastic Behavior of Cylinders

Averaged experimental values for the elastic constants of glass- or boron-epoxy cylinders are compared with theoretical values in figure 19 for the four cylinder types. Experimental elastic-constant data for individual cylinders under compressive and tensile loads are listed in table V, and calculated elastic-constant values are listed in table VI. The isotropic cylinders are characterized by approximately equal elastic properties in the longitudinal and circumferential directions whereas the orthotropic cylinders exhibit directional elastic properties. The greater stiffness of the boron-filament-reinforced composite is readily apparent from a comparison of the values of Young's modulus for boron- and glass-epoxy cylinders wound in the same manner. By comparing the experimental values for isotropic cylinders, the boron-reinforced composite was found to be about 3.5 times as stiff as the glass-reinforced composite. For the orthotropic cylinders, the boron-reinforced composite was about 4 times as stiff in the longitudinal direction and 5 times in the circumferential direction.

Calculated elastic-constant values for the four cylinder types are listed in table VI. They are graphically compared with the experimental values in figure 19. The calculated values were obtained by a complex mechanical analysis in which the properties of both matrix and reinforcement and the interaction between the two throughout a multilayer, multidirectional filament-wound cylinder were considered. In the computations, elastic constants for unidirectional layers were determined by using upper-bound calculations for random arrays of circular filaments (ref. 6). This analysis was incorporated into a computer program for multilayered, multiple-oriented layers and used successfully to predict the experimental elastic behavior of glass-epoxy filament-wound cylinders. (See ref. 7.)

In the present investigation agreement between experimental and calculated elastic-constant values was reasonably good. Experimental strain measurements used in the determination of Poisson's ratio were corrected for the increment of strain produced in the transverse portion of the gages when the gages were alined perpendicular to the direction of stressing (ref. 8). Although this correction is normally small on structural metals such as the aluminum alloys, it is significant in the Poisson strains for the orthotropic cylinders; for the orthotropic boron-epoxy cylinders, the correction was of greater magnitude than the measured strain. Experimental values for Young's modulus averaged about 15 percent greater than calculated values for glass-epoxy cylinders and about 10 percent less than calculated values for boron-epoxy cylinders. Agreement between experimental and theoretical values of shear modulus for the orthotropic

boron-epoxy cylinders was poorer than that for the other elastic moduli, the theoretical value being approximately 30 percent less than the experimental value. However, these results indicate that, in general, the present theory used to predict elastic-constant values for glass-reinforced epoxy cylinders is equally satisfactory for those reinforced with boron.

Failure of Cylinders

Each cylinder was failed by either internal pressurization, external pressurization, or axial compression. Photographs of the failed cylinders are presented in figures 20 to 32; corresponding load-strain curves to failure for each cylinder are shown in figures 33 to 40, where only absolute values of strain have been plotted; and the experimentally determined failure loads are listed in table VII. For each cylinder, the Poisson strains have signs opposite to those of the strains parallel to the direction of loading. All the cylinders subjected to internal pressure loads experienced tensile failure in the circumferential filaments. The cylinders subjected to axial compression or external pressure failed either by buckling or by a compressive mode of material failure. Cylinder failures based on the type of load to which each was subjected will be discussed subsequently. Experimental cylinder failure strengths are listed in table VIII; calculated strengths based on five methods for predicting failure are also listed. A discussion of these various methods is given in appendix B. The agreement between the experimental and calculated failure strengths listed in table VIII ranged from excellent, with discrepancies less than 5 percent, to poor, with discrepancies as great as 2100 percent. A graphical comparison of the experimental failure strengths with the most closely corresponding values calculated from the various methods is made in figure 41. The wide range of correlation shown for the various types of loading, winding pattern, and filamentary material indicates that additional research is needed before the failure strengths can be predicted with certainty.

Internal pressure failures.- The cylinders shown in figures 20 to 24 were failed by internal pressurization. Figures 20 and 21 are photographs of the two orthotropic boron-epoxy cylinders, which were the only cylinders of the same type failed under identical loading conditions. Failure occurred suddenly with a sharply defined fracture nearly perpendicular to the circumferentially wrapped filaments. An isotropic boron-epoxy cylinder is shown in figure 22. For this cylinder, failure occurred along a line approximately parallel to one set of helically wrapped filaments breaking the filaments in the opposed helical layers and the circumferential layers. All the boron-epoxy cylinders subjected to internal pressurization failed suddenly whereas failure of the glass-epoxy cylinders, shown in figures 23 and 24, occurred more gradually. The orthotropic glass-epoxy cylinder in figure 23 failed by unraveling and bulging as the pressure was increased beyond a certain value. Failure of the isotropic glass-epoxy cylinder shown in figure 24

occurred in a similar though more gradual manner. All the cylinders were porous to the extent that a bladder of some sort was required to seal against seepage leaks during pressurization. This problem was particularly acute for the orthotropic glass-epoxy cylinder, and a 1100-0 aluminum-alloy sheet liner (shown in fig. 23) was necessary before the cylinder could be effectively pressurized. The increment of pressure calculated to be carried by this aluminum liner at the cylinder failure strength was deducted from the orthotropic glass-epoxy cylinder failure pressure. Composite internal pressure failure strengths were 91.6 and 93.8 ksi (632 and 647 MN/m^2), respectively, for the two orthotropic boron-epoxy cylinders and 50.1 ksi (345 MN/m^2) for the isotropic boron-epoxy cylinder (table VIII). Comparable strengths for similar glass-epoxy cylinders were 115.0 and 68.9 ksi (793 and 475 MN/m^2). The experimental load-strain data were reduced to composite strengths by the following equation:

$$\sigma = \frac{pr(1 + \epsilon)}{t} \tag{1}$$

where for the calculation of internal pressure strength, r is taken to be the initial inside cylinder radius and ϵ is the circumferential strain at failure. The term $(1 + \epsilon)$ accounts for the increase in tensile load carried by the cylinder wall due to the increase in cylinder size under load.

By considering only the orthotropic cylinders and assuming the entire load to be carried by the circumferential filaments, the ratio of glass-filament strength in composite to boron-filament strength in composite was obtained as 422/304 = 1.39. This number may be compared with a similar ratio formed from virgin filament strengths, 700/400 = 1.75. Thus, the virgin tensile-strength advantage of glass filament over boron filament is significantly reduced when the filaments are used as reinforcement for filament-wound epoxy cylinders.

Typical load-strain curves for internal pressure failure of the orthotropic and isotropic boron-epoxy cylinders are shown in figure 33. The two orthotropic cylinders responded similarly to the pressure loads. The relationship between load and strain is linear for both the longitudinal and circumferential directions to failure. The load-strain relationship for the isotropic boron-epoxy cylinder deviated from linearity in the circumferential direction beginning at a pressure of about 0.8 ksi (5.5 MN/m^2). This deviation was accompanied by audible cracking sounds during loading. The load-strain curves for the orthotropic and isotropic glass-epoxy cylinders are similar but exhibit a small amount of nonlinear behavior prior to failure. (See fig. 34.)

External pressure failures.- The cylinders shown in figures 25 to 28 were failed by external pressurization. An orthotropic boron-epoxy cylinder is shown in figure 25 with a large hole in its side. The isotropic boron-epoxy cylinder in figure 26 contains three cracks with a common intersection. The orthotropic glass-epoxy cylinder in figure 27 appears to have undergone buckling failure. The surface is covered with minute craze

cracks, none of which were present on the surface of the cylinder before testing. The cracks exist in two separate patterns. The circumferential cracks, which are about 0.25 inch (6 mm) apart, are believed to be a consequence of axisymmetric prebuckling deformations which assume a shape similar to that of a transversely corrugated cylinder. The finer, more closely spaced oval arrays of cracks, lengthwise in the center of the cylinder and circumferentially about 120° apart, are evidence of a diamond-shaped buckle pattern. Failure occurred abruptly for all cylinders. Latex or chlorobutyl rubber external coatings were used to seal against slow fluid leaks through the porous cylinder walls. The failure area in the isotropic glass-epoxy cylinder (fig. 28) resembles a bruise on a piece of fruit. The black circumferential line segments in the failure area are pockets of the chlorobutyl rubber coating which was applied externally before testing and not completely removed before this photograph was taken.

Experimental external pressure failure strengths for orthotropic and isotropic boron-epoxy cylinders were 25.1 and 13.6 ksi (173 and 93.8 MN/m^2), respectively (table VIII). Comparable strengths for similar glass-epoxy cylinders were 19.4 and 11.5 ksi (134 and 79.3 MN/m^2). The experimental load-strain data were reduced to composite strengths by equation (1); however, for external pressure loading the radius was taken to be the outside cylinder radius. Comparison of these experimental values with those calculated by the various methods listed in table VIII indicated that only those values obtained by the shell buckling method showed reasonable agreement with the experimental values.

A survey of the load-strain curves for external pressure failure (figs. 35 to 38) indicates that all the cylinders tested buckled to some degree. The load-strain curves shown in the figures were plotted for both the circumferential and longitudinal directions for each cylinder. The possibility that buckling occurred is indicated by marked deviations from linearity, by strain reversals, or by both among gages oriented in the same direction. In figure 35, for example, where load-strain curves are plotted for external pressurization of an orthotropic boron-epoxy cylinder, external gage 6 and internal gage 4 are placed back to back in the circumferential direction. Load-strain curves from these gages are divergent as load is increased, and at a pressure of about 0.63 ksi (4.3 MN/m^2) the curves proceed in opposite directions. This divergence indicates that a depression is being formed in the surface of the cylinder at this gage location which is probably caused by circumferential buckling. Similarly, external longitudinal gage 3 indicates a strain reversal at about 0.68 ksi (4.7 MN/m^2), and its load-strain curve then converges with the curve from external longitudinal gage 2, 90° away circumferentially. This behavior suggests the possibility of a depression in the area of gage 3 and a bulge in the vicinity of gage 2 which could be caused by buckling. The load-strain curves for the remaining cylinders subjected to external pressure load are similar to those in figure 35 although variations in the severity of nonlinear deviations occur.

Axial compression failures.- The cylinders failed by axial compression are shown in figures 29 to 32. The orthotropic boron-epoxy cylinder is shown in figure 29 with failure evidenced externally by a circumferential split in the cylinder wall. The isotropic boron-epoxy cylinder in figure 30 failed around the full circumference near the bottom of the cylinder. The orthotropic glass-epoxy cylinder (fig. 31) also failed around the full circumference near the bottom. Some evidence of prebuckling deformations occurs in the form of circumferential cracks in the wall of the orthotropic glass-epoxy cylinder (fig. 31). These cracks are similar to those seen on the surface of the orthotropic glass-epoxy cylinder failed by external pressurization (fig. 28) except that here no evidence of buckling exists. Cracks were not evident on the surface of the specimen prior to testing. The failure of the isotropic glass-epoxy cylinder (fig. 32) appears similar to that exhibited by the orthotropic boron-epoxy specimen (fig. 29) with a circumferential split in the wall.

Experimental compressive failure strengths for the composite cylinders are listed in table VIII for the four cylinder types as derived from the experimental loads by using the equation

$$\sigma = \frac{P}{2\pi rt} \tag{2}$$

where r is the mean radius of the cylinder. Failure strengths for the orthotropic and isotropic boron-epoxy cylinders occurred at 24.7 and 43.3 ksi (170 and 299 MN/m^2), respectively. For glass-epoxy cylinders a fair correlation between calculated and experimental failure strengths could be made, but for the boron-epoxy cylinders the analysis yielded results as much as 9 times the experimental values. (See table VIII.)

Load-strain curves for the axial compression tests are shown in figures 39 and 40. The responses of the two boron-epoxy cylinders to load are essentially linear as shown in figure 39, and the strain-gage inputs were so nearly identical that they were averaged and plotted as single curves. The isotropic glass-epoxy cylinder (fig. 40) behaved in a manner similar to the boron-epoxy cylinders except that the strain response was nonlinear. Strain reversals, which suggested the possibility of buckling, occurred in the circumferential direction of the orthotropic glass-epoxy cylinder at an axial force of about 30 kips (136 kN).

CONCLUDING REMARKS

A study has been made to determine the mechanical behavior of multidirectional boron-epoxy and S-glass—epoxy filament-wound cylinders under tensile, compressive, torsional, and pressure loads. Young's moduli, shear moduli, and Poisson's ratios of the boron-epoxy cylinders could be predicted with reasonable accuracy by an existing

theory which had previously been used to predict elastic-constant values for glass-epoxy cylinders. The greater stiffness of the boron filament was manifested in the cylindrical composites. The stiffness of the boron-epoxy cylinders was from 350 to 500 percent greater than that of comparable glass-epoxy cylinders, the value depending on the type of filament winding pattern and the direction considered.

Each cylinder was failed by either internal pressurization, external pressurization, or axial compression. Composite failure strengths varied from 11.5 to 115 ksi (79.3 to 793 MN/m^2) for glass-reinforced cylinders and from 13.6 to 93.8 ksi (93.8 to 647 MN/m^2) for boron-reinforced cylinders. These values were dependent on the type of load and the winding pattern of the cylinder. The virgin tensile-strength advantage of glass filament over boron filament was found to be reduced significantly when tensile strengths were deduced from average failure strengths of cylinders loaded by internal pressure.

The agreement between experimental and calculated failure strengths ranged from excellent, with discrepancies less than 5 percent, to poor, with discrepancies as great as 2100 percent. Cylinders subjected to external pressurization failed by buckling, and comparison of experimental data with results calculated from an existing shell buckling theory indicated a reasonable agreement. For axial compression a nonbuckling form of material failure occurred. For glass-epoxy cylinders a fair correlation could be made between calculated and experimental failure strengths, but for the boron-epoxy cylinders the analysis yielded results as much as 9 times the experimental values. Thus, additional research is necessary before failure characteristics of multidirectional filament-wound composite cylinders, either boron- or glass-reinforced, can be accurately predicted.

Langley Research Center,
National Aeronautics and Space Administration,
Langley Station, Hampton, Va., December 12, 1968,
129-03-09-03-23.

APPENDIX A

CONVERSION OF U.S. CUSTOMARY UNITS TO SI UNITS

The International System of Units (SI) was adopted by the Eleventh General Conference on Weights and Measures, Paris, October 1960, in Resolution No. 12 (ref. 4). Conversion factors for the units used herein are given in the following table:

Physical quantity	U.S. Customary Unit	Conversion factor (*)	SI Unit
Force	kip = 1000 lbf	4.448×10^3	newtons (N)
Length	in.	2.54×10^{-2}	meters (m)
Moduli and stress . . .	ksi = 1000 lbf/in^2	6.895×10^6	newtons per square meter (N/m^2)
Temperature	(^{o}F + 459.67)	5/9	degrees Kelvin (^{o}K)
Density	lbm/in^3	2.768×10^4	kilograms per cubic meter (kg/m^3)

*Multiply value given in U.S. Customary Unit by conversion factor to obtain equivalent value in SI Unit.

Prefixes to indicate multiple of units are as follows:

Prefix	Multiple
micro (μ)	10^{-6}
milli (m)	10^{-3}
centi (c)	10^{-2}
kilo (k)	10^3
mega (M)	10^6
giga (G)	10^9

APPENDIX B

CALCULATION OF CYLINDER FAILURE STRENGTHS

Eight theoretical methods have been used to calculate the failure strengths of filament-wound cylinders. A comparison is made in table VIII of these calculated strengths with the experimental strengths for the four cylinder types under three loading conditions. In figure 41 the experimentally determined failure strengths are compared with the most closely corresponding failure strengths calculated by the various methods. The excellent-to-poor agreement between experimental and calculated values shown for the various types of loading, winding pattern, and filamentary material indicates that additional research is needed before cylinder failure strengths can be predicted with certainty.

Many investigators have proposed using the various forms of a stress-interaction equation for anisotropic materials to calculate the failure strengths of composite materials. These equations are usually based on conditions at the onset of yielding rather than those at failure so that, from a theoretical standpoint, the interaction equations are misapplied. Nevertheless, the use of the interaction equations is representative of the present state of the art for predicting failure in composite structures. A classic example of these equations is the anisotropic yield criterion presented by Hill (ref. 9), which for a state of plane stress and transverse isotropy reduces to

$$\left(\frac{\sigma_L}{X}\right)^2 - \frac{\sigma_L \sigma_T}{X^2} + \left(\frac{\sigma_T}{Y}\right)^2 + \left(\frac{\tau_{LT}}{S}\right)^2 = 1 \tag{B1}$$

where σ_L and σ_T are normal stresses, τ_{LT} is the shear stress in a layer associated with directions parallel and perpendicular to the filaments, X and Y are allowable strengths of the same unidirectional layer in directions parallel and perpendicular to the filaments, and S is an allowable shearing strength of the layer.

Another form of anisotropic yield criterion is

$$\left(\frac{\sigma_L}{X}\right)^2 - \frac{\sigma_L \sigma_T}{XY} + \left(\frac{\sigma_T}{Y}\right)^2 + \left(\frac{\tau_{LT}}{S}\right)^2 = 1 \tag{B2}$$

which differs from equation (B1) only by the denominator of the second term. This form has been suggested by several investigators as an empirical fit to test data. (See ref. 10.) Unfortunately, equation (B2) has also been erroneously attributed to Hill as his anisotropic yield criterion (refs. 11 and 12, for example).

Still another form of an anisotropic yield criterion, the ANC-18 interaction criterion, is

$$\left(\frac{\sigma_L}{X}\right)^2 + \left(\frac{\sigma_T}{Y}\right)^2 + \left(\frac{\tau_{LT}}{S}\right)^2 = 1 \tag{B3}$$

which differs from both (B1) and (B2) in that the cross-product term is omitted. This form was proposed in reference 13 for the design of wood structures.

The three anisotropic yield criteria discussed (eqs. (B1) to (B3)) can be used to calculate the failure strength of any single anisotropic, unidirectional layer of composite material. In a multilayered composite not all layers will necessarily fail simultaneously. As one or several of the layers have failed, the layers which are still intact may be able to sustain the existing load. As the load is increased, the still-intact layers reach an ultimate strength at which failure occurs. In the present calculations, since the test cylinders had two types of layers, helical- and circumferential-wound, upper and lower bounds of the strength of the multilayered cylinder were established by assuming that failure occurred in one type of layer while the other remained intact. Presumably, then, the strength of a multilayered cylinder should lie between these two failure strengths. The elastic stress distributions for each layer of a multilayered, anisotropic composite material as developed in reference 12 were used for determining these bounds, which are tabulated in table VIII for all three yield criteria.

The failure strengths X and Y of a unidirectional layer in directions parallel and perpendicular to the filaments and a shearing strength S used in evaluating equations (B1) to (B3), are listed in table IX for the boron-epoxy and glass-epoxy materials of this investigation. Tension values for X are based on the tensile strengths of 5.75-inch (14.6-cm) diameter NOL-rings (ref. 3) adjusted to the appropriate filament volume fractions (table IV). Compression values for X are taken from reference 14, which presents test data for 0.5-inch (1.27-cm) diameter unidirectional tubes with a filament volume fraction of 0.50. No adjustment is made to these values because no information is available concerning the effect of volume fraction on compressive strength. Tension values for Y are assumed to be equal to the tensile ultimate strength of the resin as determined from tests of cast bars (fig. 6). Compression values for Y are based on compressive-strength results reported in reference 12 for circumferentially wrapped glass-epoxy tubes. The change from glass to boron filaments is assumed to have a negligible effect on the Y strength. The values for S are based on average torsion-test results reported in reference 15 for circumferentially wrapped glass-epoxy tubes. Shear strengths of the unidirectional layer are also assumed to be independent of glass or boron filaments and volume fraction.

Internal Pressure Failure Strength

Strength calculations made for the four cylinder types under internal pressurization with floating end closures reveal several interesting points. Hill's anisotropic yield criterion (eq. (B1)) and the ANC-18 interaction criterion (eq. (B3)) give the same failure strength predictions within 1 percent for any particular loading condition of the boron-epoxy and glass-epoxy materials considered. This result is attributed to the negligible

contribution made by the cross-product term in equation (B1), which is primarily due to the large magnitude of the X-strength value compared with the Y-strength value. The strength bound associated with failure of the circumferential layer gives the best agreement with the experimental failure strengths; however, this is a lower bound for the boron composites and an upper bound for the glass composites. The change from lower to upper bound is related to changes in the stress distributions in the layers for a large difference in the stiffness of boron and glass filaments. The difference between bounds associated with the failure of circumferential or helical layers varies from 50 to 300 percent of the lower bound which makes prediction of the failure rather vague but does permit a reasonable correlation with the experimental data after the experiment has been performed. Thus, for internal pressure failure strengths, calculations based on Hill's criterion for the failure of the circumferential layer (eq. (B1)) or the ANC-18 method (eq. (B3)) give the best correlation with experimental values of the six anisotropic yield criteria considered. Values calculated by either method are within ±5 percent of the experimental values for glass-epoxy cylinders and within -18 percent of those for boron-epoxy cylinders. (See table VIII.)

External Pressure Failure Strength

For all the cylinder types, external pressurization with floating end closures resulted in buckling instability of the cylinder wall. Buckling strengths were calculated by using the shell buckling equation of reference 12 for a simply supported, multilayered orthotropic cylinder loaded by external pressure. The results are listed in table VIII. The magnitude of the experimental buckling strengths is small, and calculated values range from -15 to +25 percent of these values.

Compressive instability strengths are a function of wall thickness, cylinder diameter, and elastic stiffnesses of the various layers. For certain dimensions and stiffnesses, calculations based on anisotropic yield criteria may indicate that compressive instability occurs at strengths greater than other failure criteria might predict. Calculated external pressure failure strengths based on the six forms of anisotropic yield criteria (eqs. (B1) to (B3)) are listed in table VIII. These calculated strengths are from 2 to 9 times greater than both the experimental failure strengths and the calculated buckling strengths of the four cylinders.

Included in table VIII is another failure criterion based on the hypothesis that when the strain in the direction of loading reaches the compressive yield strain for the epoxy-resin matrix (fig. 6) the individual filaments will lose their resistance to compressive loading and the composite material will fail. The calculated strengths at which the matrix yields for the four cylinder types are also listed in table VIII. These values are 4 to 21 times greater than the shell buckling strength.

Thus, the shell buckling method is selected as the criterion for cylinder failure under external pressurization, and good agreement is shown with the experiments both in mode of failure and magnitude of strength.

Axial Compressive Strength

Axial compressive loading produced failures of the cylinder wall material in three of the four cylinders. The fourth, the orthotropic glass-epoxy cylinder, gave a slight indication of shell buckling (fig. 40). Failure predictions for axial compression based on calculations of the six anisotropic yield criteria, a shell buckling method, and a matrix-yielding method do not indicate any clear-cut choice of method. (See table VIII.)

For the one cylinder that indicated buckling, the calculated buckling strength is 27 percent greater than the experimental value and is between the lower and upper bounds calculated by the various anisotropic yield criteria. For the isotropic glass-epoxy cylinder, the calculated buckling strength is 70 percent greater than the experimental value and 90 percent greater than the largest of the calculated upper bounds. For the two boron-epoxy cylinders, calculated buckling strengths are 2.5 to 3 times the experimental failure strength, and one calculated strength is above the upper bound whereas the other is below the lower bound for the anisotropic yield criteria.

Failure strengths calculated by the matrix-yielding method show the best correlation with the experimental failure strengths for the two glass-epoxy cylinders but are 5 to 10 times higher for the two boron-epoxy cylinders. A comparison of failure strengths obtained from Hill's anisotropic yield criterion (eq. (B1)) with experimental values indicates two experimental values well below the lower calculated bound, one experimental value above the upper bound, and one experimental value midway between bounds. No obvious correlation exists.

The best recommendation that can be made for prediction of axial compressive strength is to select either the lowest value calculated by the shell buckling or matrix-yielding method or the upper bound of Hill's anisotropic yield criterion. Additional research is needed to improve the analysis of failure strengths for multilayered, anisotropic composite cylinders loaded in axial compression.

REFERENCES

1. Herring, Harvey W.: Selected Mechanical and Physical Properties of Boron Filaments. NASA TN D-3202, 1966.

2. Herring, Harvey W.; and Krishna, V. Gopala: Shear Moduli of Boron Filaments. NASA TM X-1246, 1966.

3. Baucom, Robert M.: Tensile Behavior of Boron-Filament-Reinforced Epoxy Rings and Belts. NASA TN D-5053, 1969.

4. Comm. on Metric Pract.: ASTM Metric Practice Guide. NBS Handbook 102, U.S. Dep. Com., Mar. 10, 1967.

5. Dow, Norris F.; and Rosen, B. Walter: Evaluations of Filament-Reinforced Composites for Aerospace Structural Applications. NASA CR-207, 1965.

6. Hashin, Zvi; and Rosen, B. Walter: The Elastic Moduli of Fiber-Reinforced Materials. Trans. ASME, Ser. E: J. Appl. Mech., vol. 31, no. 2, June 1964, pp. 223-232.

7. Card, Michael F.: Experiments to Determine Elastic Moduli for Filament-Wound Cylinders. NASA TN D-3110, 1965.

8. Baumberger, R.; and Hines, F.: Practical Reduction Formulas for Use on Bonded Wire Strain Gages in Two-Dimensional Stress Fields. Proc. of Soc. Exp. Stress Anal., vol. II, no. 1, 1944, pp. 113-127.

9. Hill, R.: The Mathematical Theory of Plasticity. The Clarendon Press, 1950, pp. 318-319.

10. Tsai, Stephen W.: Strength Characteristics of Composite Materials. NASA CR-224, 1965, pp. 6-7.

11. Calcote, L. R.; and Grimes, G. C.: Investigation of Structural Design Concepts for Fibrous Aircraft Structures. AFFDL-TR-67-29-Vol. II, U.S. Air Force, Jan. 1967, p. 137. (Available from DDC as AD 813394.)

12. Card, Michael F.: Experiments to Determine the Strength of Filament-Wound Cylinders Loaded in Axial Compression. NASA TN D-3522, 1966.

13. Anon.: Design of Wood Aircraft Structures. ANC-18 Bull., Second ed., Munitions Board Aircraft Comm., Dep. Defense, June 1951.

14. Davis, John G., Jr.: Fabrication of Uniaxial Filament-Reinforced Epoxy Tubes for Structural Applications. Paper presented at 14th National SAMPE Symposium (Cocoa Beach, Fla.), Nov. 5-7, 1968.

15. Dexter, H. Benson: Correlation of Three Standard Shear Tests for Unidirectional Glass-Epoxy Composites. M. S. Thesis, Virginia Polytech. Inst., 1967.

TABLE I.- REPRESENTATIVE PROPERTIES OF MATERIALS USED IN THIS INVESTIGATION

Material	Ultimate tensile strength		Young's modulus		Poisson's ratio	Density	
	ksi	GN/m^2	ksi	GN/m^2		lbm/in^3	kg/m^3
Boron filament	[a]400	[a]2.8	[b]65 000	[b]450	0.20	0.11	3.0×10^3
S-glass filament	700	4.8	12 000	83	.20	.09	2.5
Epoxy	7.6	.052	475	3.28	.35	.043	1.19

[a]Obtained from reference 3.

[b]Obtained from reference 1.

TABLE II.- AVERAGE CYLINDER WALL THICKNESSES

Cylinder type	Axial compression		Internal pressure		External pressure	
	in.	mm	in.	mm	in.	mm
Orthotropic boron[a]	0.054	1.4	0.050	1.3	0.046	1.2
			.049	1.2		
Isotropic boron	.043	1.1	.038	1.0	.039	1.0
Orthotropic glass	.097	2.5	.099	2.5	.099	2.5
Isotropic glass	.082	2.1	.084	2.1	.088	2.2

[a]Two orthotropic boron cylinders were failed by internal pressurization.

TABLE III.- AVERAGE CYLINDER WALL DENSITIES

Cylinder type	Axial compression		Internal pressure		External pressure	
	lbm/in^3	kg/m^3	lbm/in^3	kg/m^3	lbm/in^3	kg/m^3
Orthotropic boron[a]	0.079	2190	0.083	2300	0.093	2570
Isotropic boron	.083	2300	.087	2410	.089	2460
Orthotropic glass	.060	1660	.063	1740	.062	1720
Isotropic glass	.058	1610	.058	1610	.061	1690

[a]Two orthotropic boron cylinders were failed by internal pressurization. The wall density for only one of these was determined.

TABLE IV.- AVERAGE CYLINDER COMPONENT VOLUME FRACTIONS

Cylinder type	Axial compression			Internal pressure			External pressure		
	V_f	V_r	V_v	V_f	V_r	V_v	V_f	V_r	V_v
Orthotropic boron[a]	0.45	0.39	0.16	0.45	0.48	0.07	0.55	0.41	0.04
Isotropic boron	.45	.49	.06	.48	.48	.04	.48	.54	Undeterminable
Orthotropic glass	.41	.56	.03	.42	.58	0	.41	.56	.03
Isotropic glass	.41	.51	.08	.39	.52	.09	.40	.55	.05

[a]Two orthotropic boron cylinders were failed by internal pressurization. Volume fractions for only one of these were determined.

TABLE V.- EXPERIMENTAL ELASTIC CONSTANTS FOR BORON-EPOXY AND GLASS-EPOXY FILAMENT-WOUND CYLINDERS

(a) U.S. Customary Units

Cylinder type	$E_{x,t}$, ksi	$E_{x,c}$, ksi	$E_{y,t}$, ksi	$E_{y,c}$, ksi	G_{xy}, ksi	$\mu_{xy,t}$	$\mu_{xy,c}$	$\mu_{yx,t}$	$\mu_{yx,c}$
Orthotropic boron	10×10^3	9.8×10^3	22×10^3	18×10^3	0.70×10^3	0.049	0.039	0.039	---
	12	11	27	26	1.0	.025	.037	.065	0.16
	12	11	21	21	.99	.020	.053	.034	.09
Average	12	11	23	22	.90	.031	.043	.048	.13
Isotropic boron	10×10^3	10×10^3	9.3×10^3	8.9×10^3	4.0×10^3	0.41	0.42	0.37	0.39
	11	12	10	9.2	4.9	.40	.37	.37	.35
	10	11	9.1	8.1	4.4	.35	.41	.36	.32
Average	10	11	9.4	8.7	4.4	.39	.40	.37	.35
Orthotropic glass	2.8×10^3	2.8×10^3	4.3×10^3	4.2×10^3	0.58×10^3	0.097	0.12	0.13	0.11
	2.9	3.1	4.4	4.8	.54	.12	.12	.15	.14
Average	2.9	3.0	4.4	4.5	.56	.11	.12	.14	.13
Isotropic glass	2.3×10^3	2.7×10^3	2.4×10^3	2.7×10^3	0.95×10^3	0.35	0.35	0.39	0.33
	2.7	2.8	2.3	2.8	1.1	.36	.35	.35	.34
	2.8	3.0	2.9	3.1	1.1	.35	.40	.37	.38
Average	2.6	2.8	2.5	2.9	1.1	.35	.37	.37	.35

(b) International System of Units

Cylinder type	$E_{x,t}$, GN/m^2	$E_{x,c}$, GN/m^2	$E_{y,t}$, GN/m^2	$E_{y,c}$, GN/m^2	G_{xy}, GN/m^2	$\mu_{xy,t}$	$\mu_{xy,c}$	$\mu_{yx,t}$	$\mu_{yx,c}$
Orthotropic boron	69	68	150	120	4.8	0.049	0.039	0.039	---
	83	76	190	180	6.9	.025	.037	.065	0.16
	83	76	140	140	6.8	.020	.053	.034	.09
Average	78	73	160	150	6.2	.031	.043	.048	.13
Isotropic boron	69	69	63	61	28	0.41	0.42	0.37	0.39
	76	83	69	63	34	.40	.37	.37	.35
	69	76	63	56	30	.35	.41	.36	.32
Average	71	76	65	60	31	.39	.40	.37	.35
Orthotropic glass	19	19	30	29	4.0	0.097	0.12	0.13	0.11
	20	21	30	33	3.7	.12	.12	.15	.14
Average	20	20	30	31	3.9	.11	.12	.14	.13
Isotropic glass	16	19	17	19	6.6	0.35	0.35	0.39	0.33
	19	19	16	19	7.6	.36	.35	.35	.34
	19	21	20	21	7.6	.35	.40	.37	.38
Average	18	20	18	20	7.3	.35	.37	.37	.35

TABLE VI.- CALCULATED ELASTIC CONSTANTS FOR BORON-EPOXY AND GLASS-EPOXY FILAMENT-WOUND CYLINDERS

(a) U.S. Customary Units

Cylinder type	E_x, ksi	E_y, ksi	G_{xy}, ksi	μ_{xy}	μ_{yx}
Orothotropic boron	11×10^3	21×10^3	0.56×10^3	0.022	0.042
Isotropic boron	9.5	11	4.6	.35	.40
Orthotropic glass	2.5	4.0	.41	.08	.13
Isotropic glass	2.1	2.4	.96	.33	.37

(b) International System of Units

Cylinder type	E_x, GN/m^2	E_y, GN/m^2	G_{xy}, GN/m^2	μ_{xy}	μ_{yx}
Orthotropic boron	76	145	3.9	0.022	0.042
Isotropic boron	66	76	32	.35	.40
Orthotropic glass	17	28	2.8	.08	.13
Isotropic glass	14	17	6.6	.33	.37

TABLE VII.- EXPERIMENTAL FAILURE LOADS FOR THE FOUR CYLINDER TYPES UNDER THREE LOADING CONDITIONS

Cylinder type	Axial compression		Internal pressure		External pressure	
	kips	kN	ksi	MN/m^2	ksi	MN/m^2
Orthotropic boron[a]	12.8	57.0	3.04	21.0	0.746	5.14
			3.05	21.0		
Isotropic boron	17.8	79.2	1.26	8.69	.345	2.38
Orthotropic glass	43.4	193	7.43	51.3	1.20	8.28
Isotropic glass	34.4	153	3.73	25.7	.638	4.40

[a]Two orthotropic boron cylinders were failed by internal pressurization.

TABLE VIII.- COMPARISON OF EXPERIMENTAL AND CALCULATED FAILURE STRENGTHS FOR THE FOUR CYLINDER TYPES UNDER THREE LOADING CONDITIONS

(a) U.S. Customary Units

Loading	Cylinder type	Composite failure strength, ksi								
		Experimental	Calculated						Shell buckling method	Matrix-yielding method
			Anisotropic yield criteria							
			Eq. (B1)		Eq. (B2)		Eq. (B3)			
			Circumferential	Helical	Circumferential	Helical	Circumferential	Helical		
Internal pressure[a]	Orthotropic boron	91.6	75.3	115.3	80.9	113.4	75.0	115.6		
		93.8	----	----	----	----	----	----		
	Isotropic boron	50.1	41.2	82.2	39.5	83.4	41.4	82.3		
	Orthotropic glass	115.0	109.1	27.0	148.1	26.8	108.0	26.8		
	Isotropic glass	68.9	71.6	23.0	62.0	23.2	72.1	23.0		
External pressure	Orthotropic boron	25.1	204.4	159.4	235.6	158.1	204.4	159.4	31.6	531.0
	Isotropic boron	13.6	105.9	106.6	98.4	107.2	106.6	106.6	11.6	238.6
	Orthotropic glass	19.4	136.9	40.2	176.9	39.8	134.4	40.2	19.0	86.2
	Isotropic glass	11.5	91.6	29.9	80.9	30.2	92.8	29.9	10.0	50.9
Axial compression	Orthotropic boron	24.7	89.1	106.6	89.1	124.7	89.3	105.6	64.6	229.0
	Isotropic boron	43.3	82.2	104.7	72.8	115.3	82.8	104.5	132.0	202.0
	Orthotropic glass	46.0	25.5	74.1	25.4	97.2	25.5	73.0	58.6	54.3
	Isotropic glass	43.4	24.3	37.0	23.4	38.9	24.3	37.0	73.8	48.4

[a]Two orthotropic boron cylinders were failed by internal pressurization; however, calculations were made for only one as the volume fractions were not determined for the other.

(b) International System of Units

Loading	Cylinder type	Composite failure strength, MN/m^2								
		Experimental	Calculated						Shell buckling method	Matrix-yielding method
			Anisotropic yield criteria							
			Eq. (B1)		Eq. (B2)		Eq. (B3)			
			Circumferential	Helical	Circumferential	Helical	Circumferential	Helical		
Internal pressure[a]	Orthotropic boron	632	519	795	558	782	517	797		
		647	----	----	----	----	----	----		
	Isotropic boron	345	284	567	272	575	285	567		
	Orthotropic glass	793	752	186	1021	185	745	185		
	Isotropic glass	475	494	159	427	160	497	159		
External pressure	Orthotropic boron	173	1409	1099	1624	1090	1409	1099	218	3661
	Isotropic boron	94	730	735	678	739	735	735	80	1645
	Orthotropic glass	134	944	277	1220	274	927	277	131	594
	Isotropic glass	79	632	206	558	208	640	206	69	351
Axial pressure	Orthotropic boron	170	614	735	614	860	616	728	445	1578
	Isotropic boron	299	567	722	502	795	571	721	910	1393
	Orthotropic glass	317	176	511	175	670	176	503	404	374
	Isotropic glass	299	168	255	161	268	168	255	509	334

[a]Two orthotropic boron cylinders were failed by internal pressurization; however, calculations were made for only one as the volume fractions were not determined for the other.

TABLE IX.- FAILURE STRENGTHS OF UNIDIRECTIONAL COMPOSITE LAYER OF BORON-EPOXY OR GLASS-EPOXY USED IN THE FAILURE-STRENGTH CALCULATIONS FOR THE MULTILAYERED CYLINDERS

Cylinder loading	Cylinder type	Unidirectional strengths					
		X		Y		S	
		ksi	MN/m^2	ksi	MN/m^2	ksi	MN/m^2
Tension	Orthotropic boron	111	760	8	55	9	62
	Isotropic boron	119	820	↓	↓	↓	↓
	Orthotropic glass	178	1230				
	Isotropic glass	165	1140				
Compression	Orthotropic boron	309	2130	12	83	9	62
	Isotropic boron	309	2130	↓	↓	↓	↓
	Orthotropic glass	207	1430				
	Isotropic glass	207	1430				

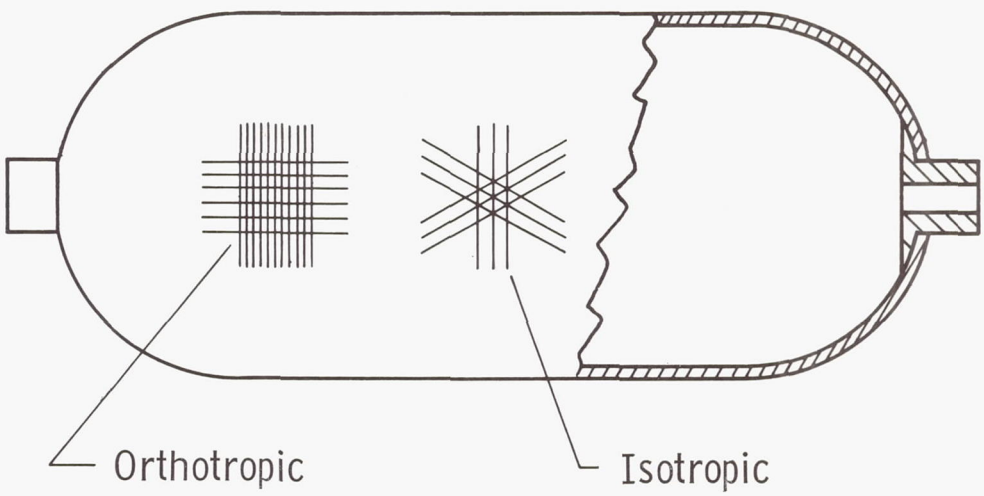

Figure 1.- Filament winding patterns.

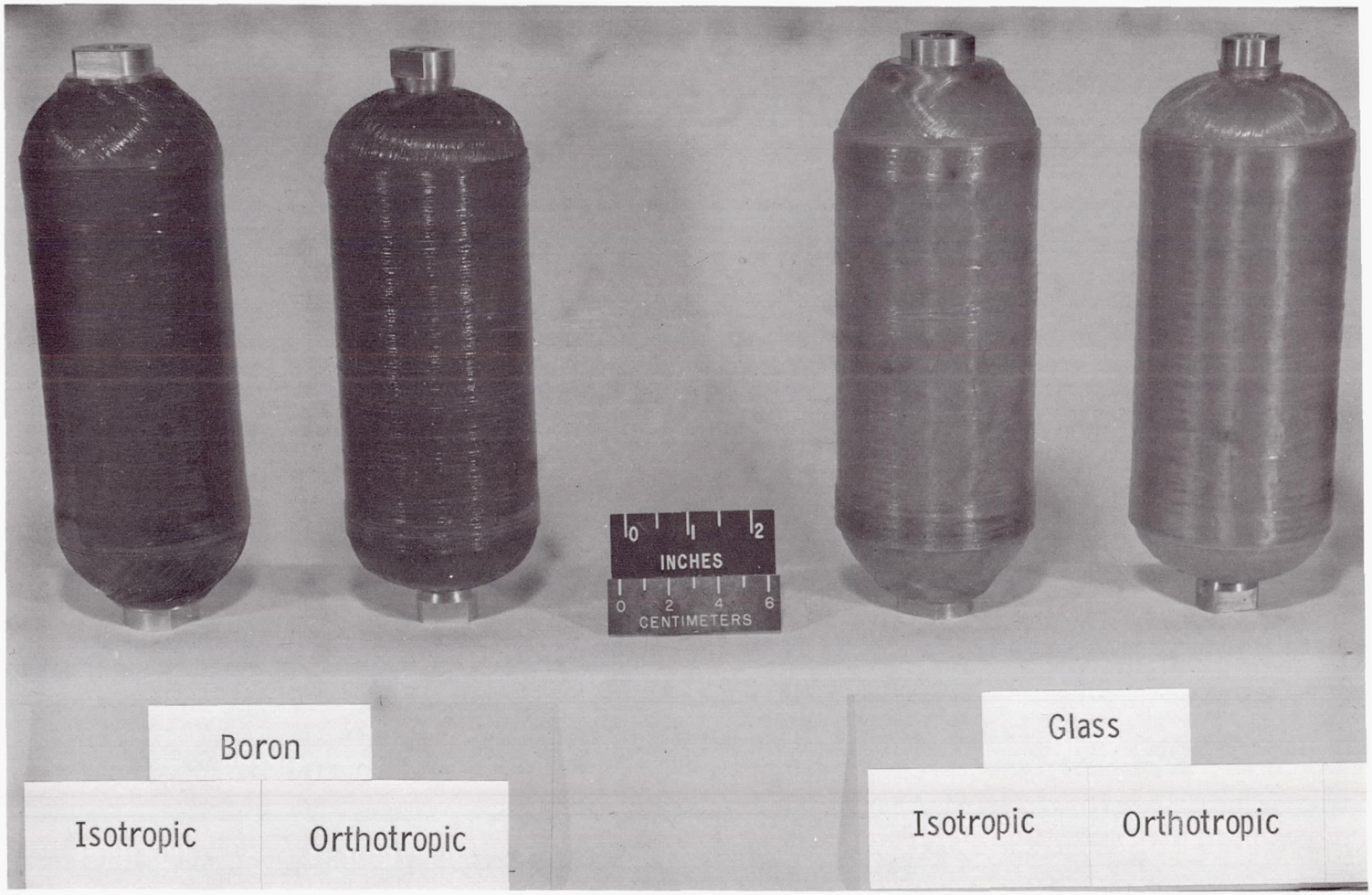

Figure 2.- Boron-epoxy and glass-epoxy filament-wound bottles. L-65-9167.1

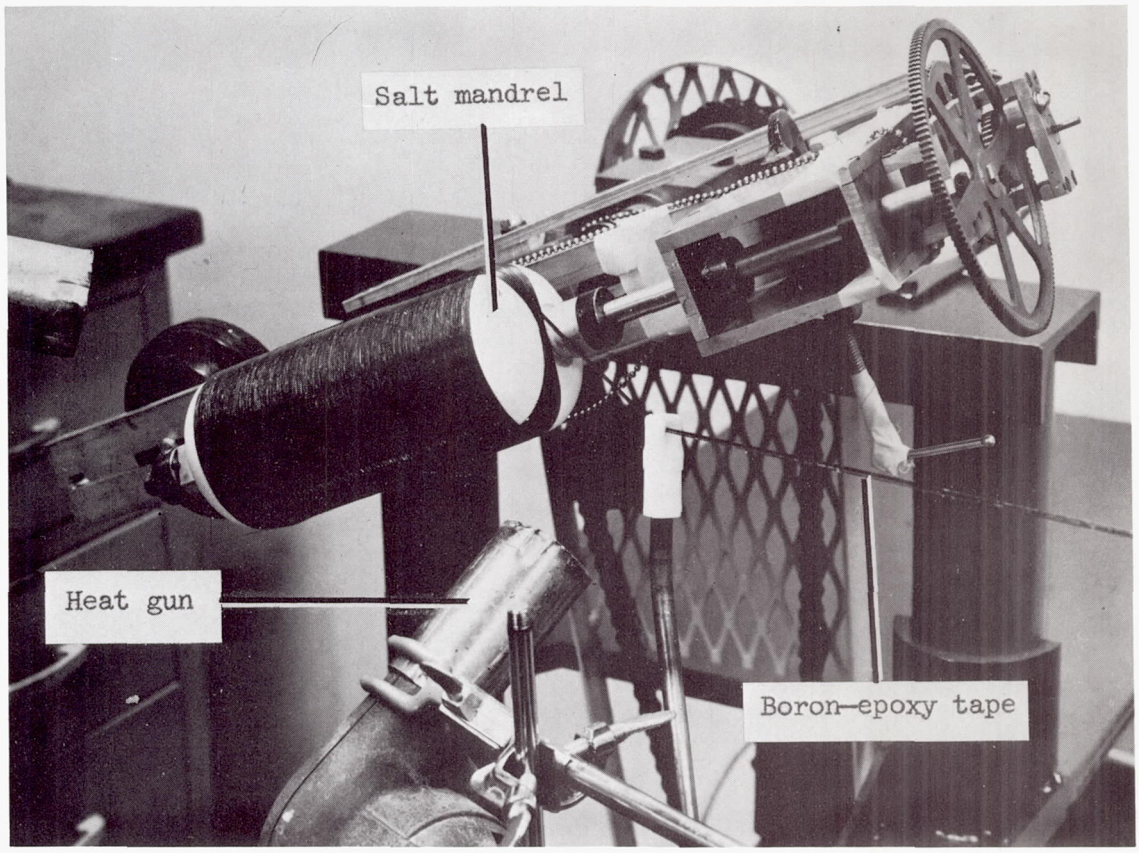

Figure 3.- Longitudinal winding of boron-epoxy tape onto a salt mandrel. L-68-10,069

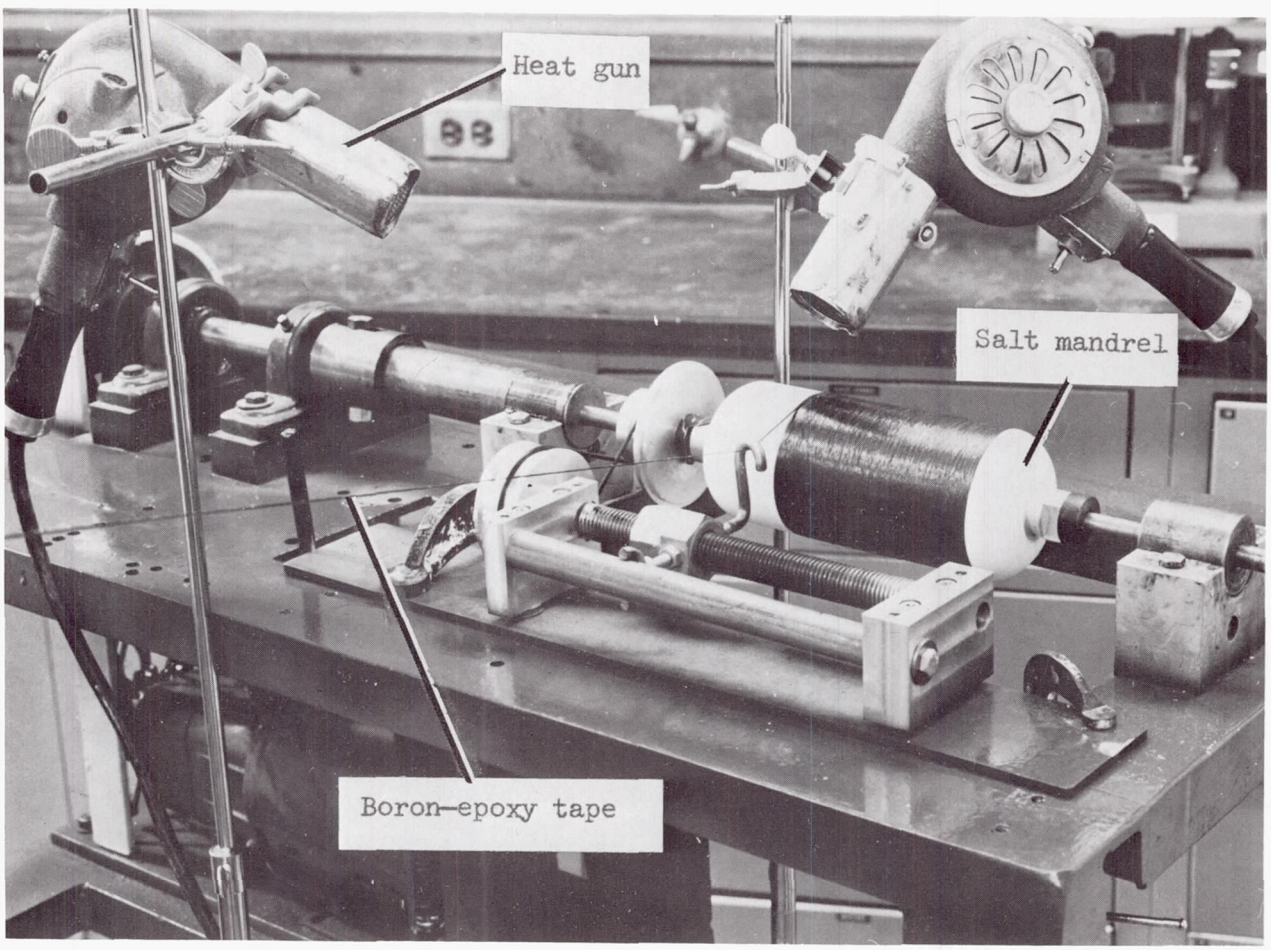

Figure 4.- Circumferential winding of boron-epoxy tape onto a salt mandrel. L-68-10,070

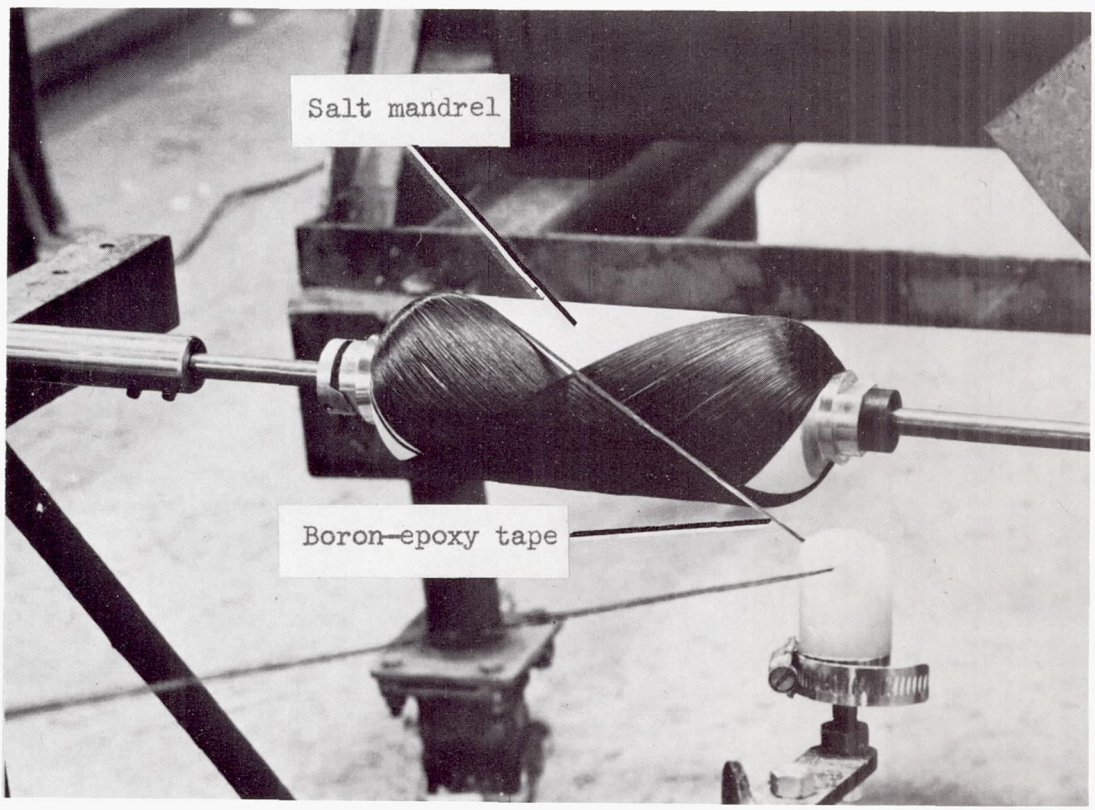

Figure 5.- Helical winding of boron-epoxy tape onto a salt mandrel. L-68-10,071

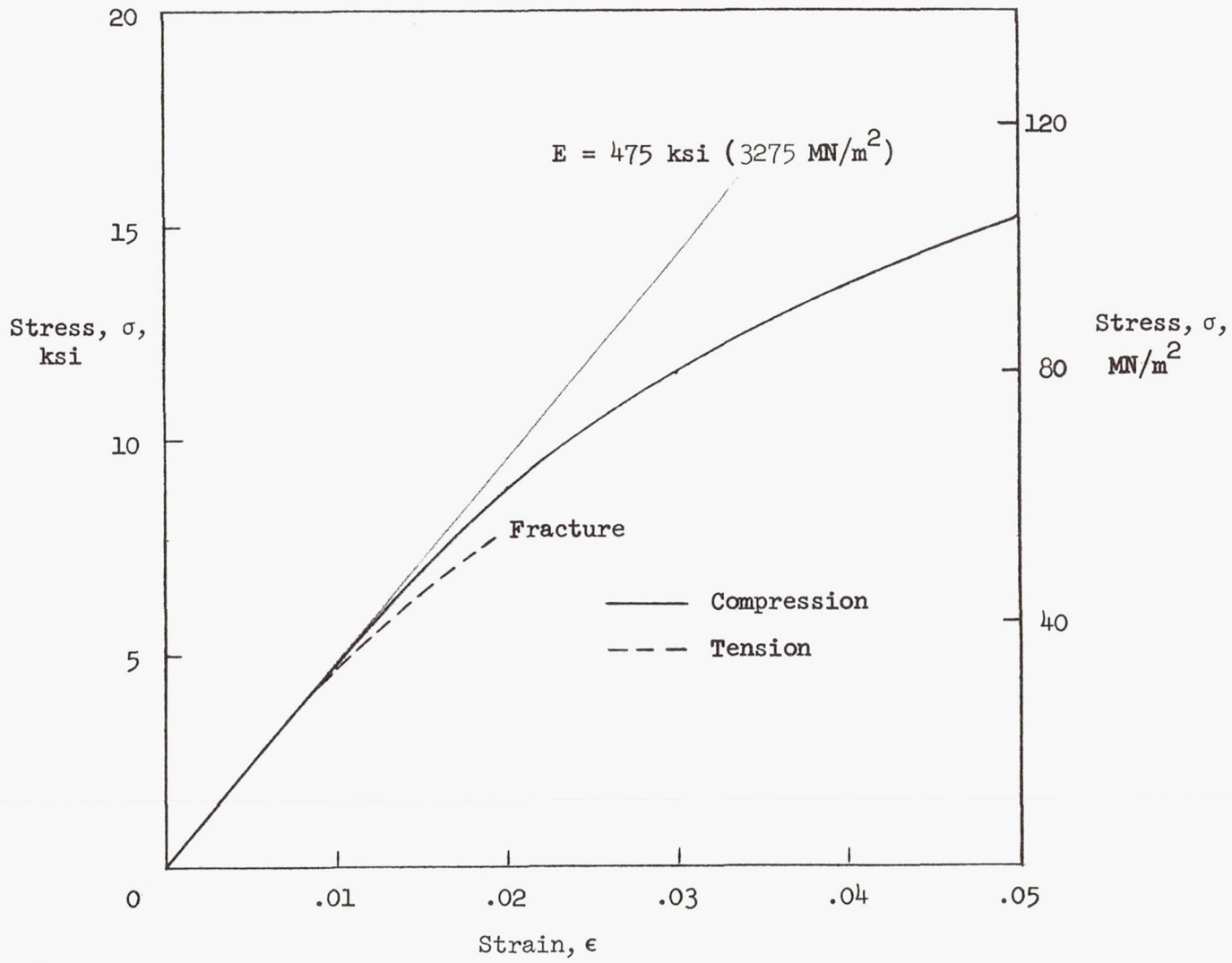

Figure 6.- Stress-strain curves for epoxy resin system used herein.

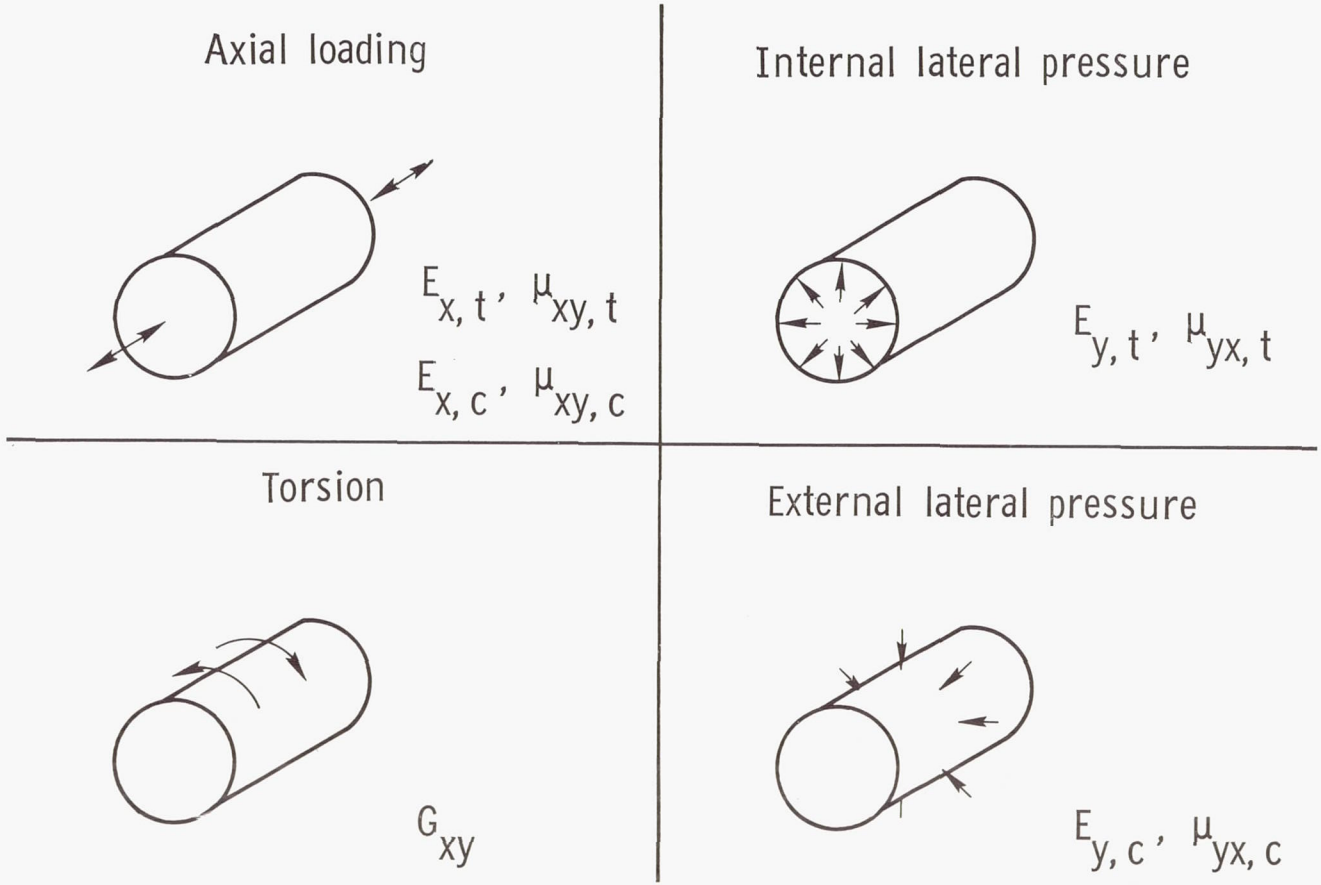

Figure 7.- Cylinder loading for determination of elastic constants.

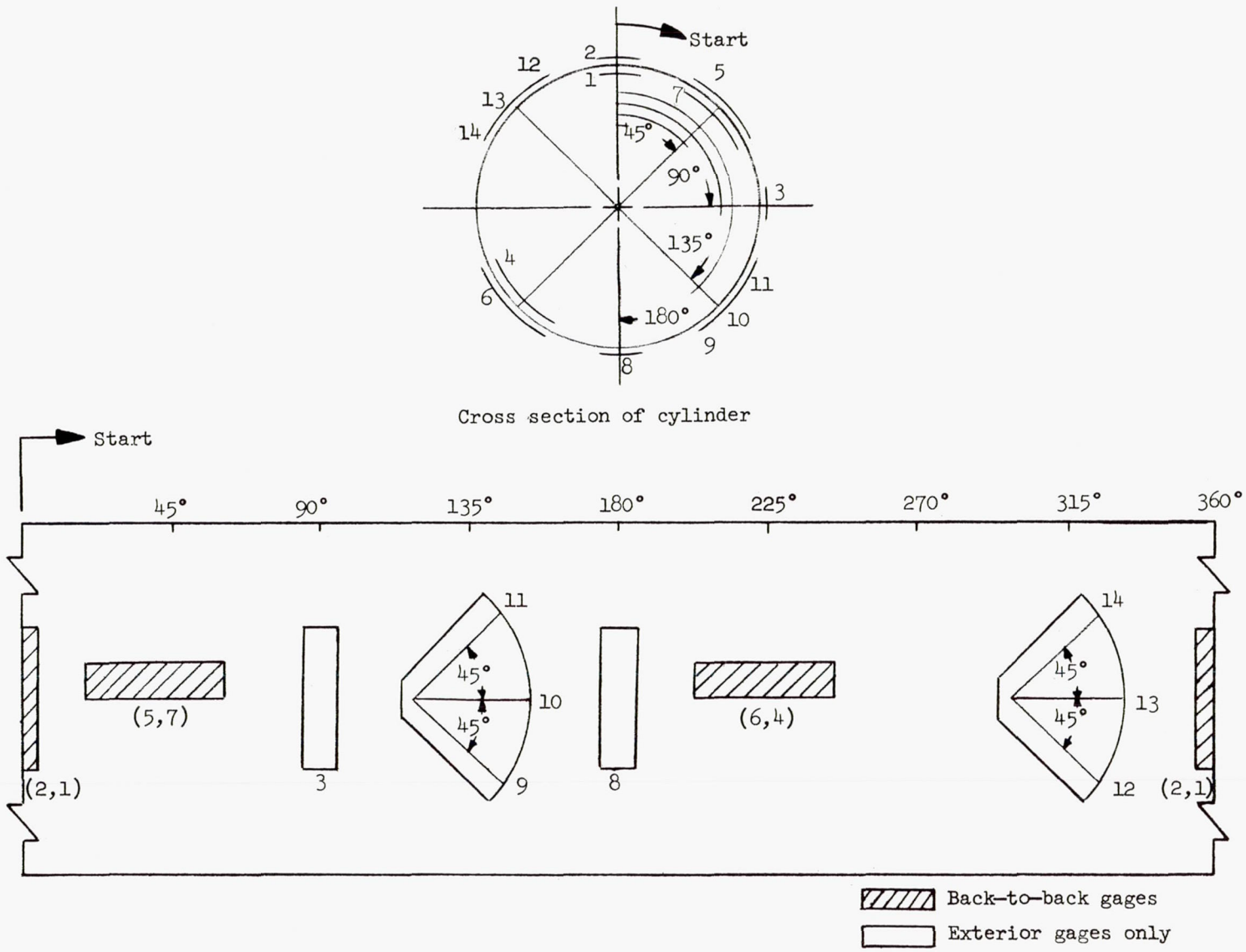

Figure 8.- Location of wire strain gages on the cylinder surface.

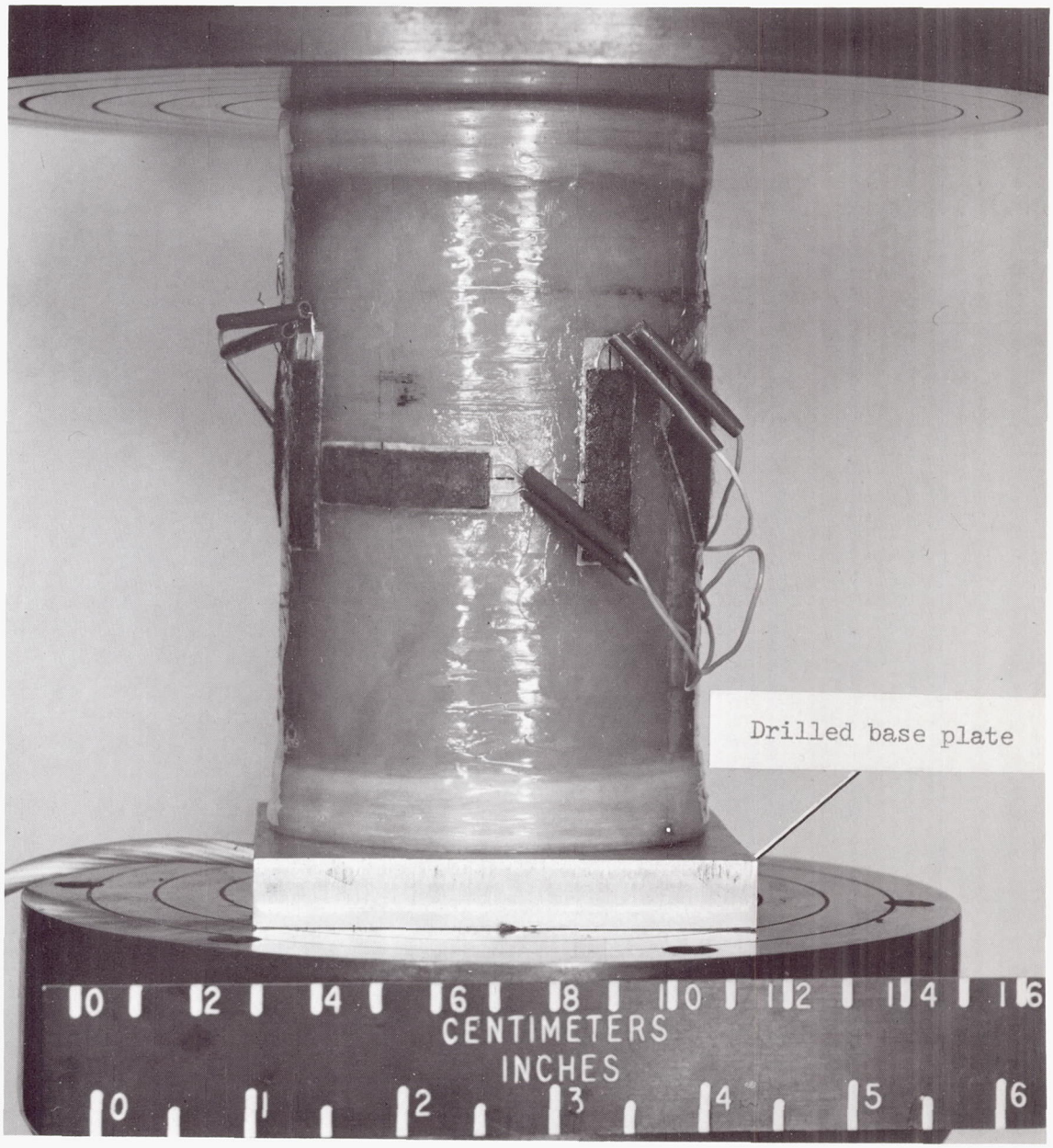

Figure 9.- Axial compression test of an isotropic glass-epoxy cylinder. L-67-2936.1

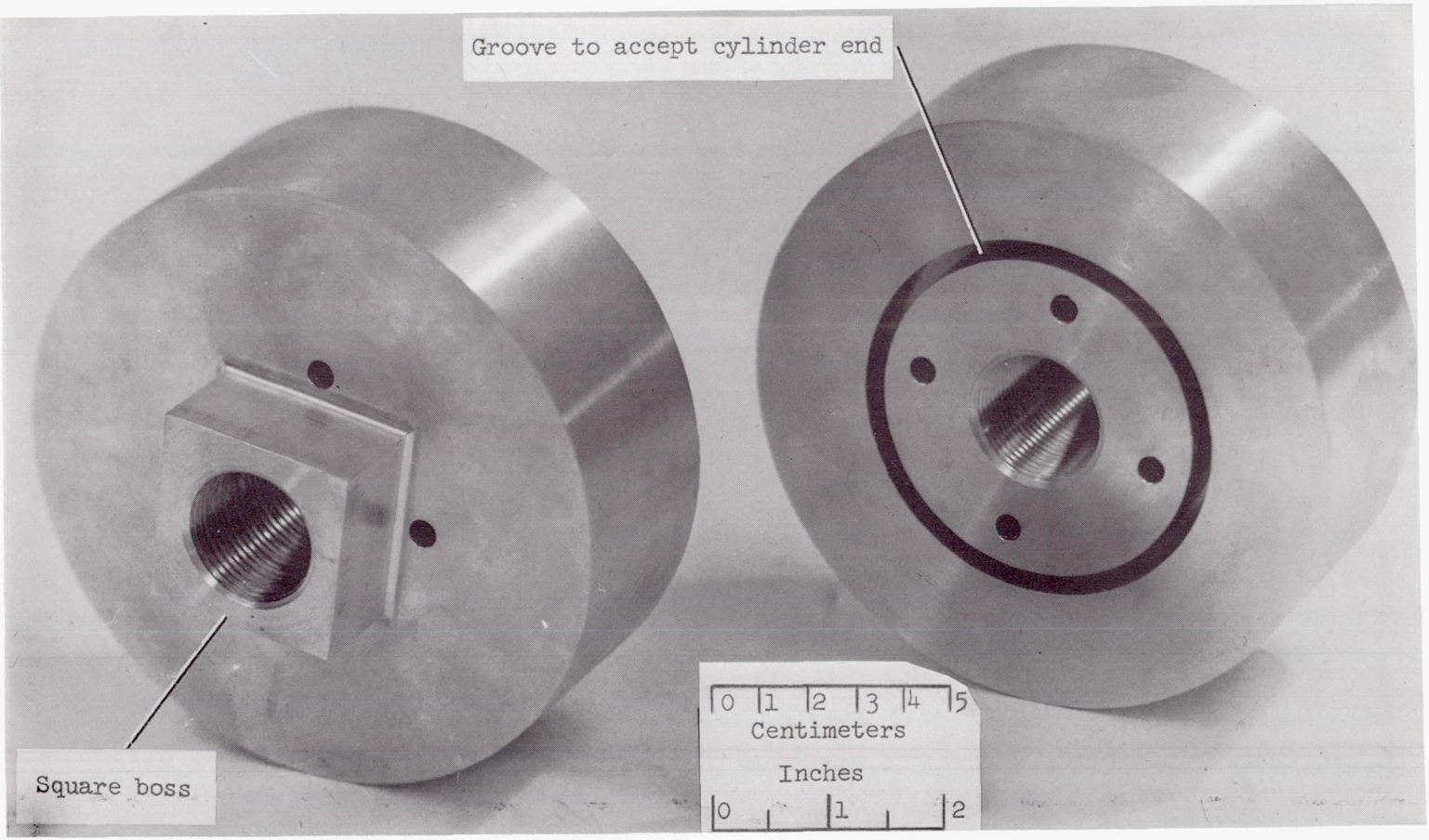

Figure 10.- Fixtures for tension and torsion testing of cylinders.

L-67-3579.1

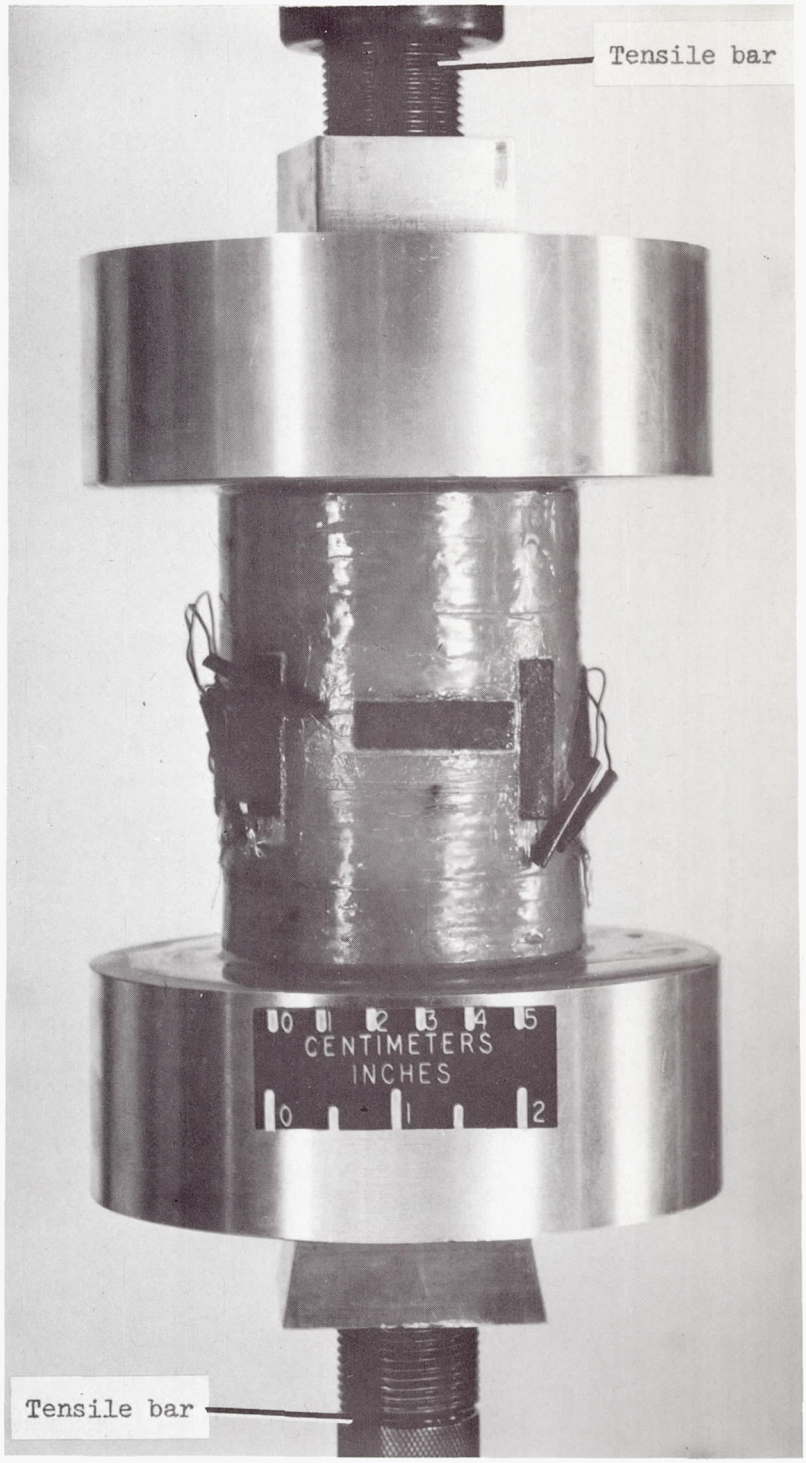

Figure 11.- Axial tension test of an isotropic glass-epoxy cylinder. L-67-2947.1

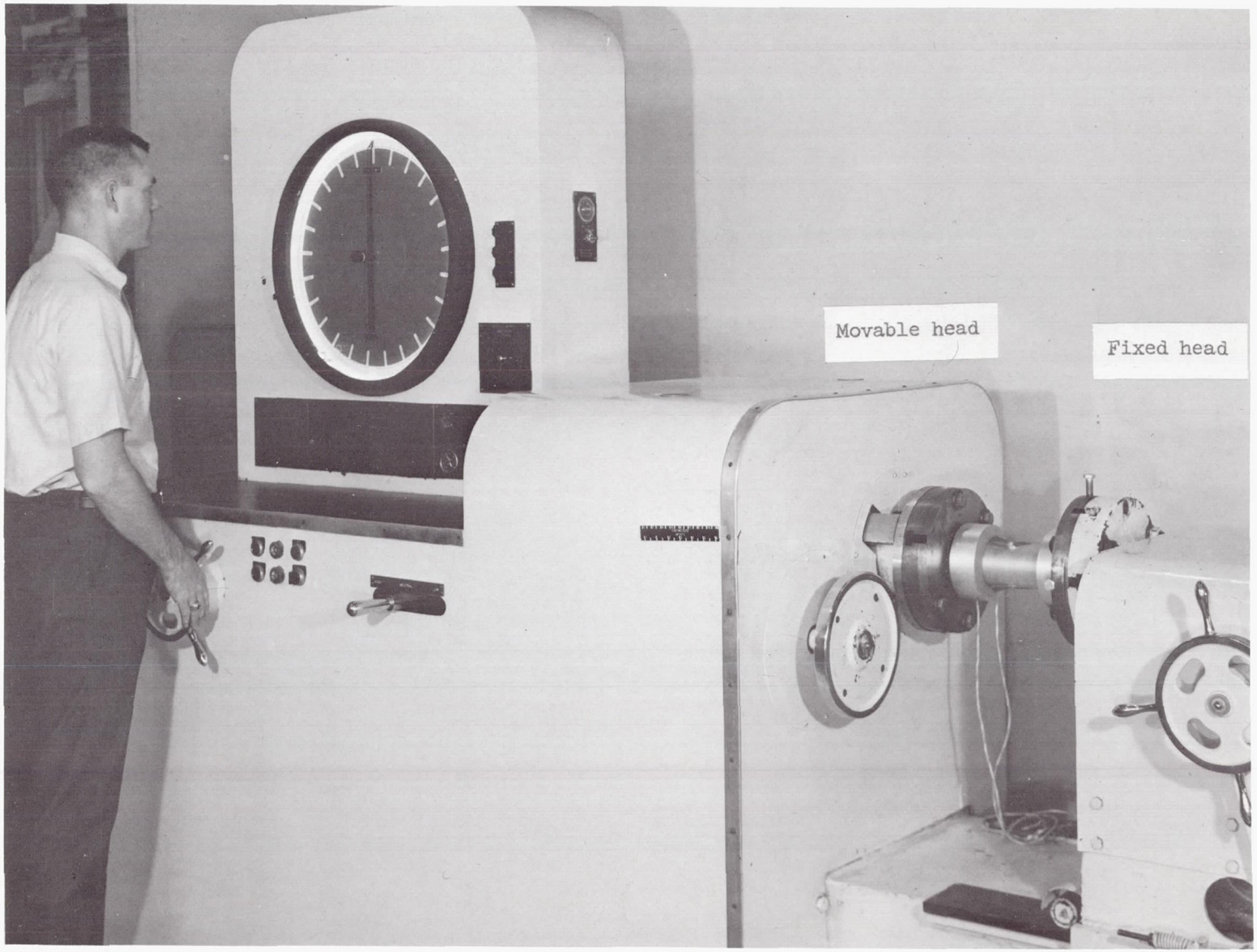

Figure 12.- Torsion test of an isotropic glass-epoxy cylinder. L-67-2423.1

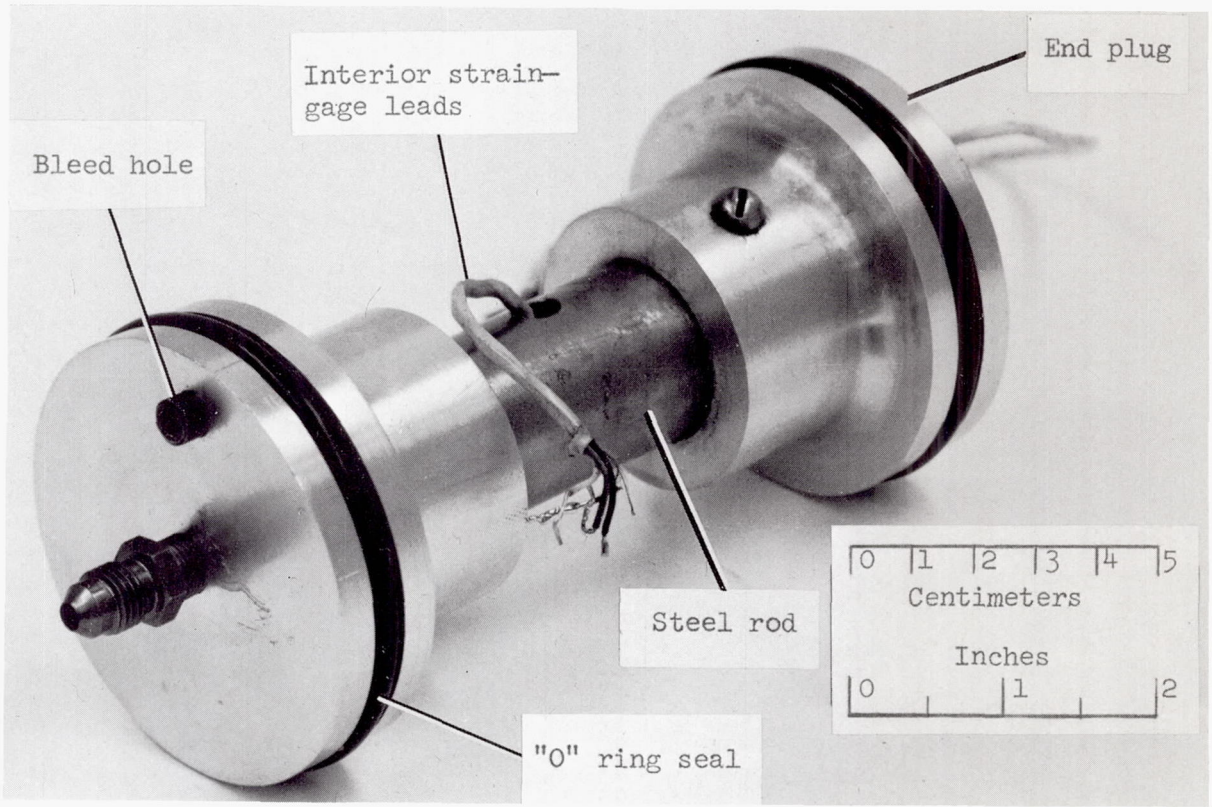

Figure 13.- Fixture for internal pressure testing of cylinders. L-67-3582.1

Test fixture of figure 13

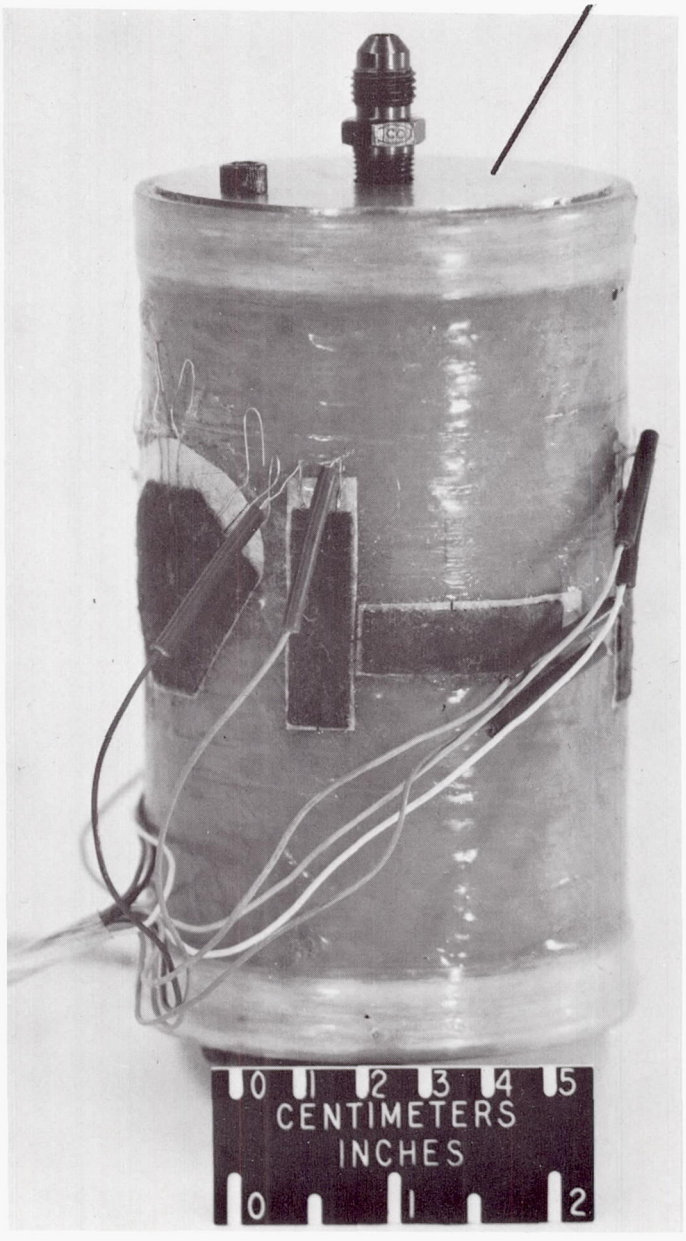

Figure 14.- An isotropic glass-epoxy cylinder with fixture for internal pressure testing inserted. L-67-3580.1

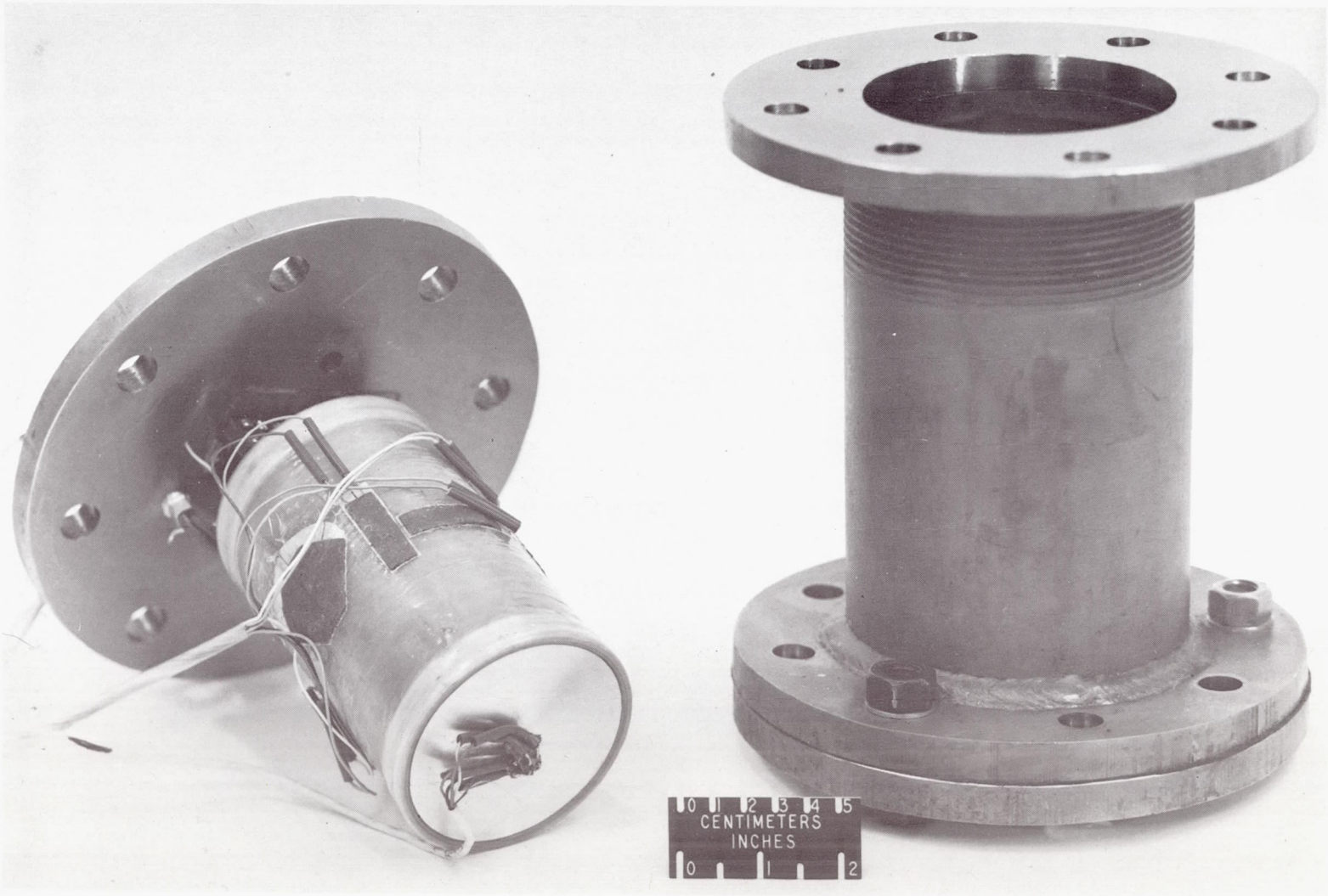

Figure 15.- Glass-epoxy cylinder before insertion in chamber for external pressure testing. L-67-3581

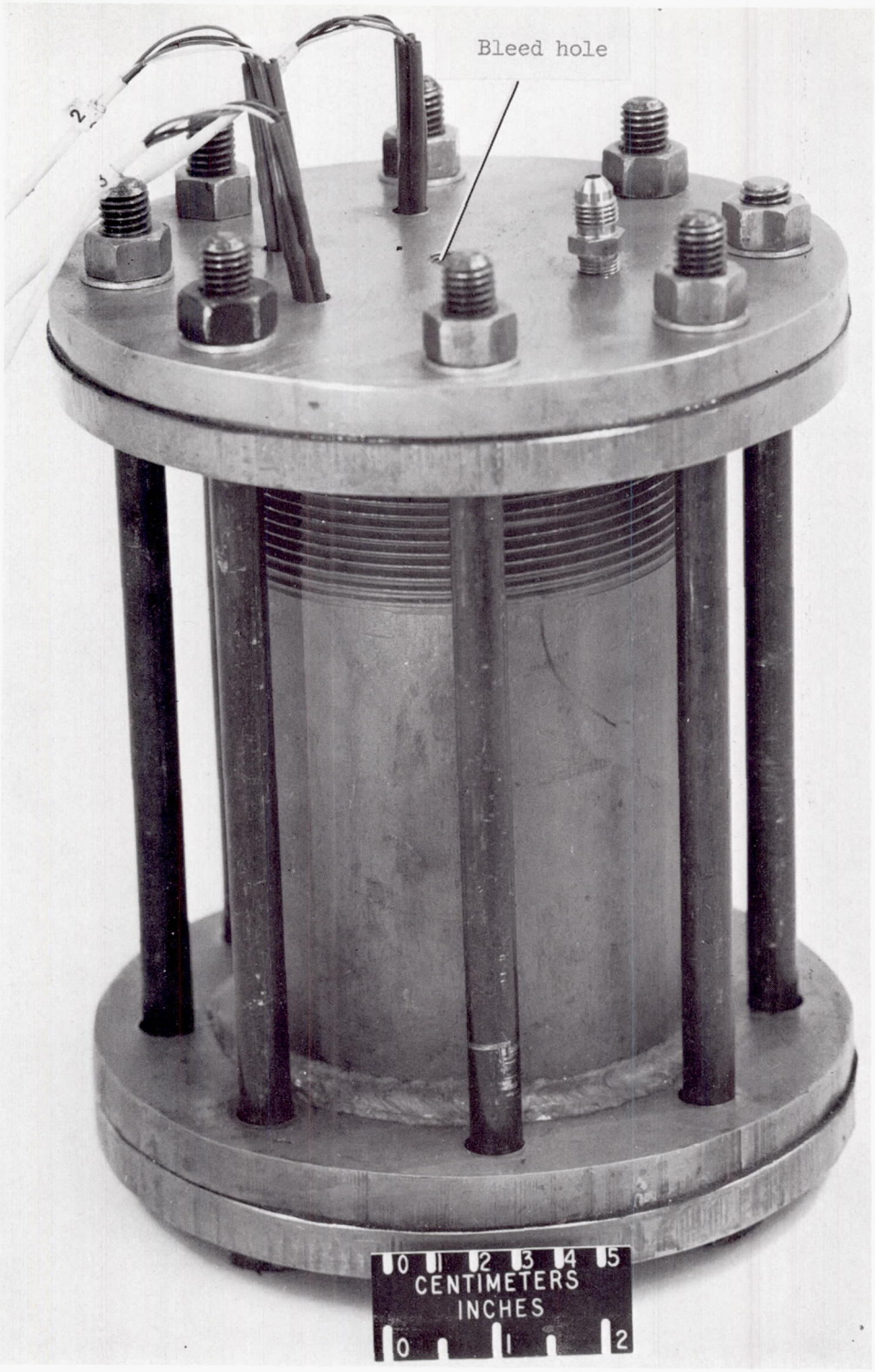

Figure 16.- Closed chamber with cylinder specimen inside ready for external pressure testing. L-67-3583.1

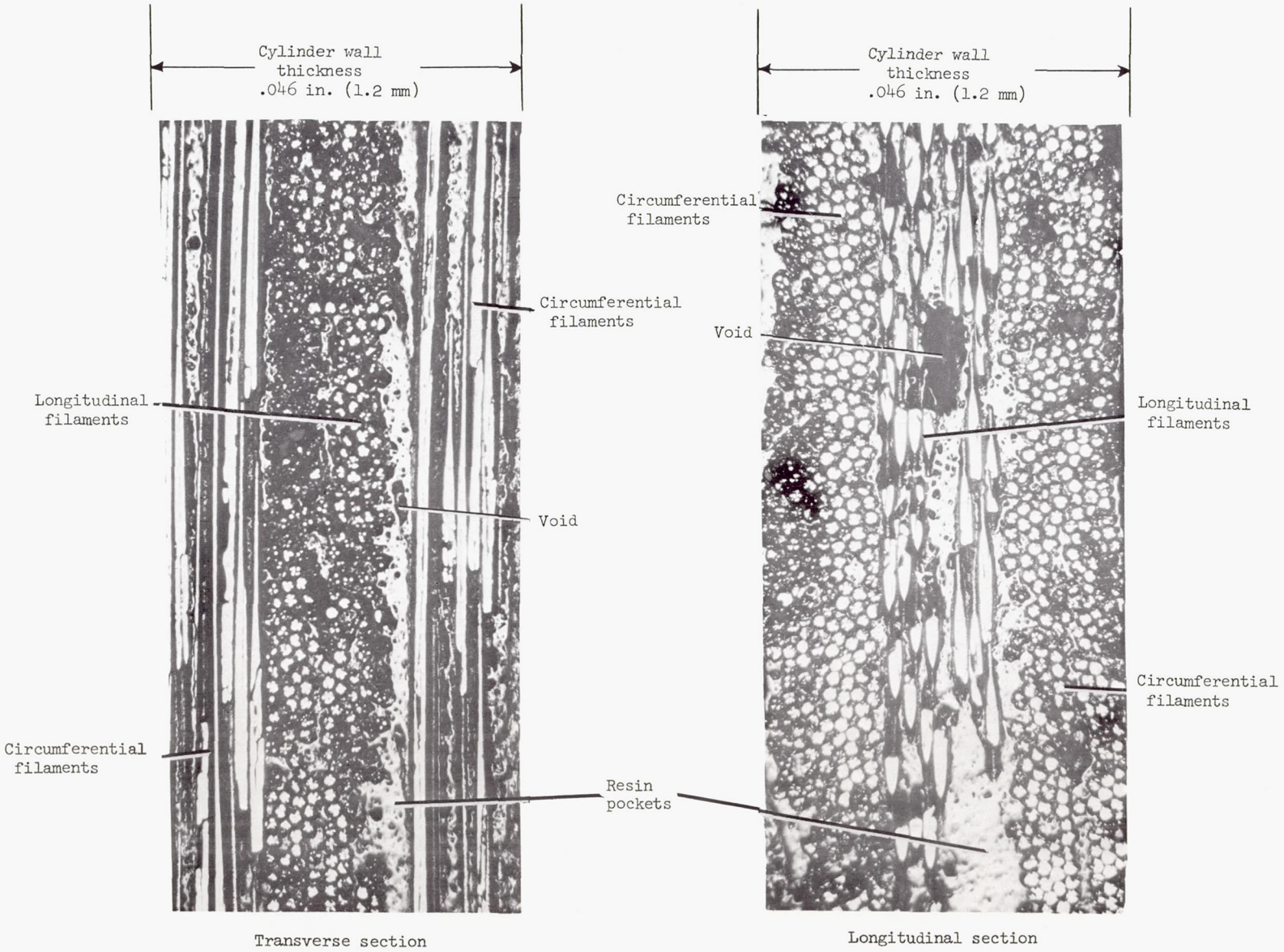

Figure 17.- Typical sections from an orthotropic boron-epoxy cylinder wall.

L-68-10,072

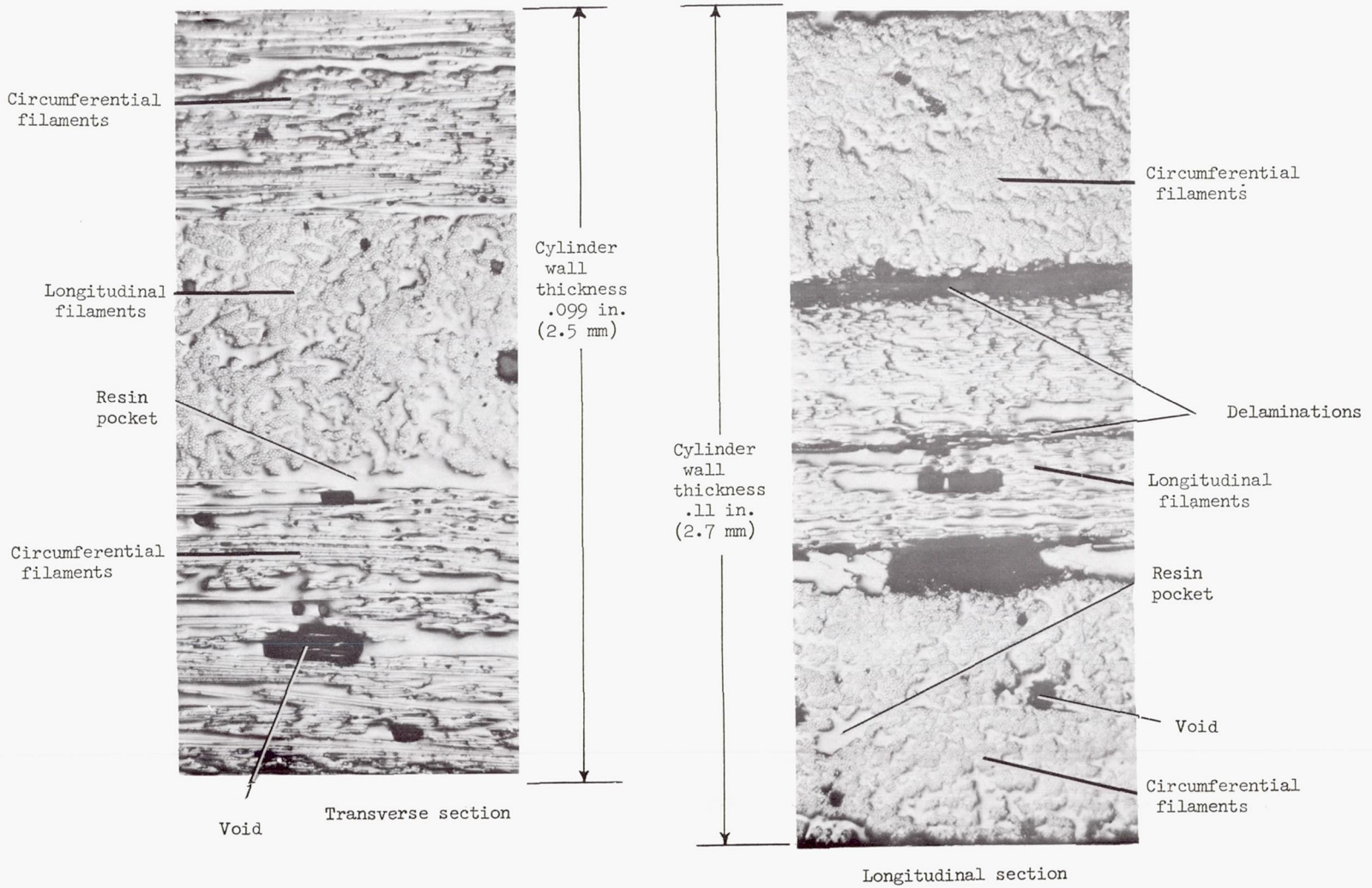

Figure 18.- Typical sections from an orthotropic glass-epoxy cylinder wall. L-68-10,073

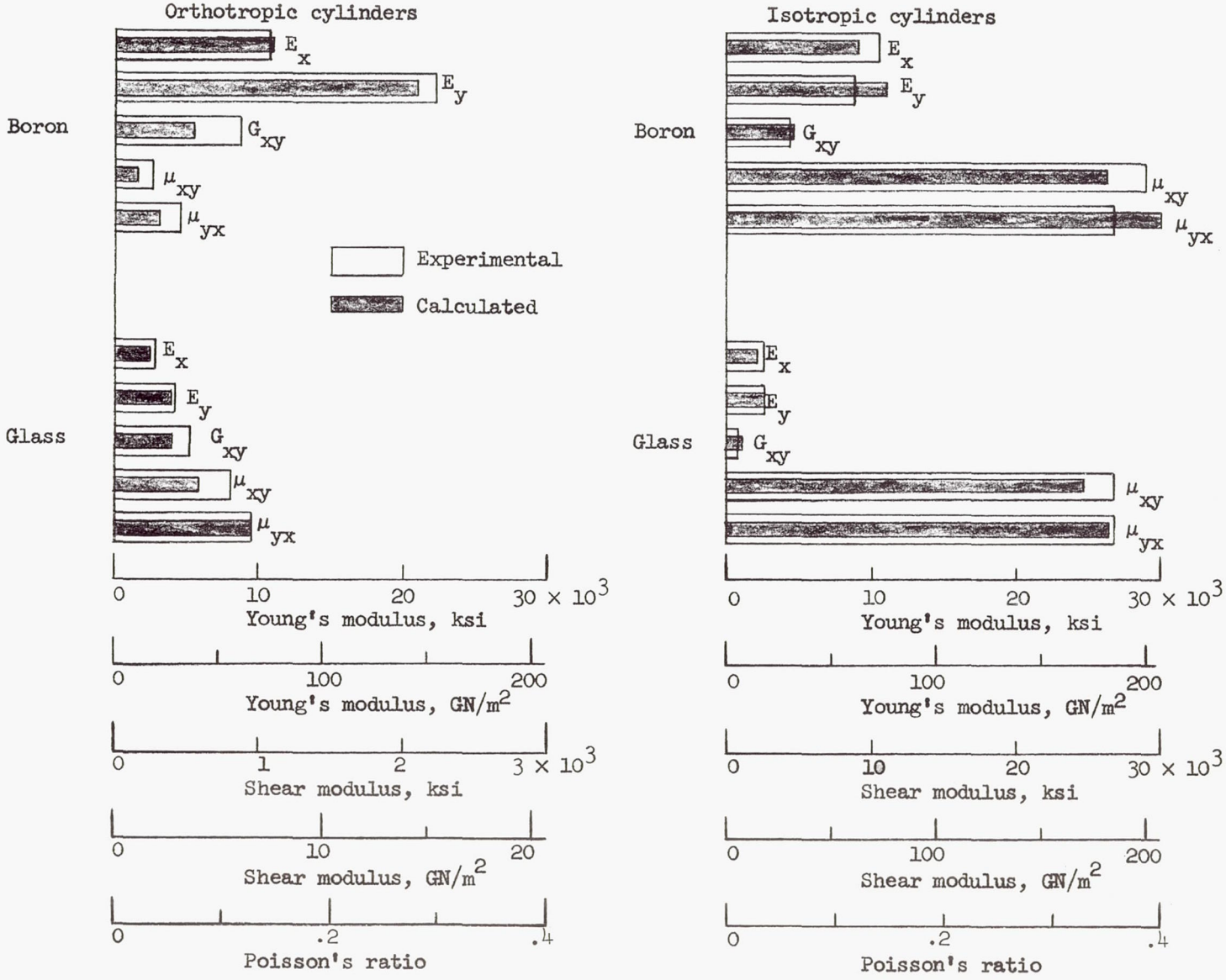

Figure 19.- Comparison of average experimental and calculated elastic constants for boron-epoxy or glass-epoxy filament-wound cylinders.

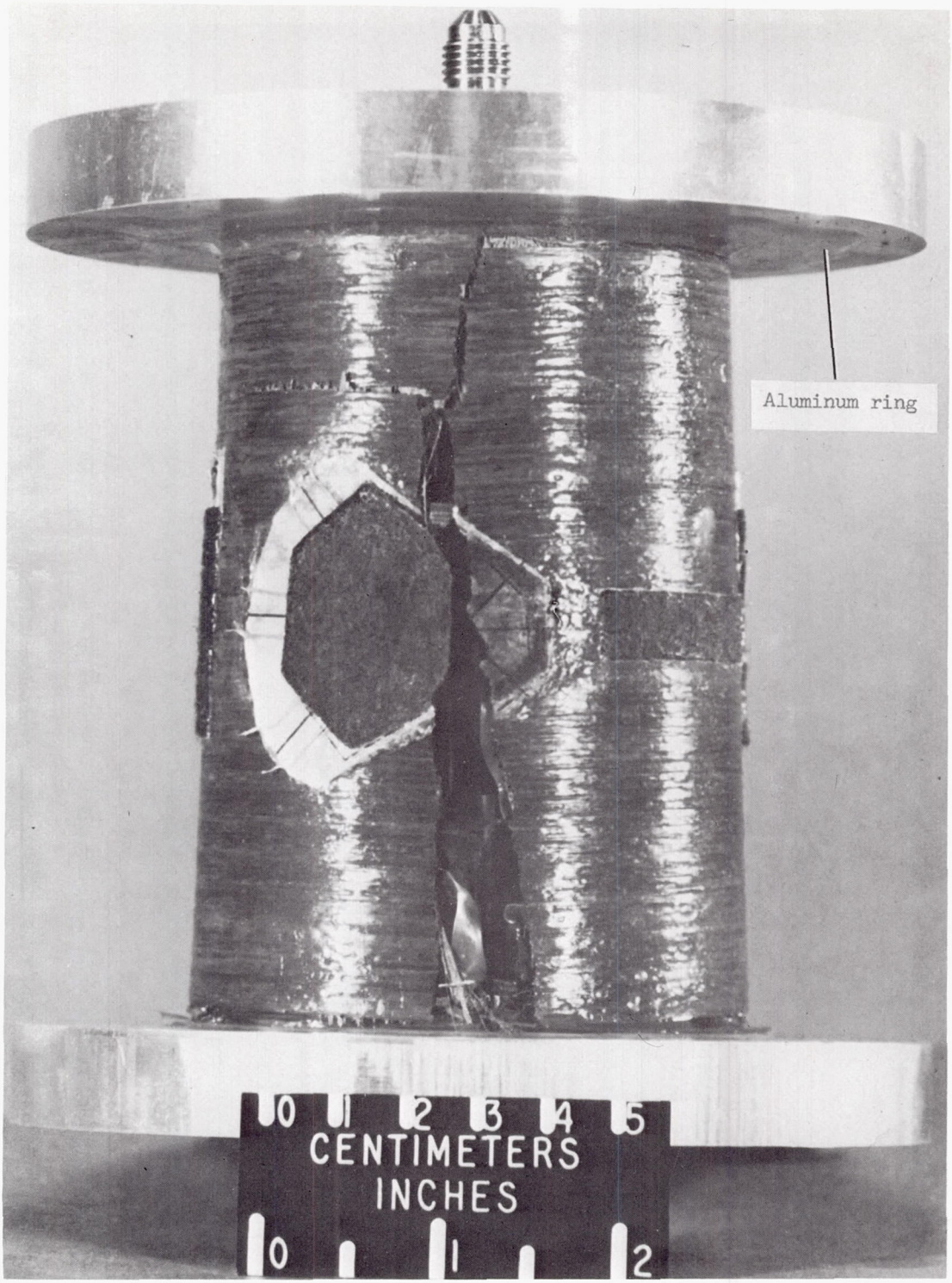

Figure 20.- Orthotropic boron-epoxy cylinder failed by internal pressurization. L-66-5700.1

Figure 21.- Second orthotropic boron-epoxy cylinder failed by internal pressurization. L-67-3214

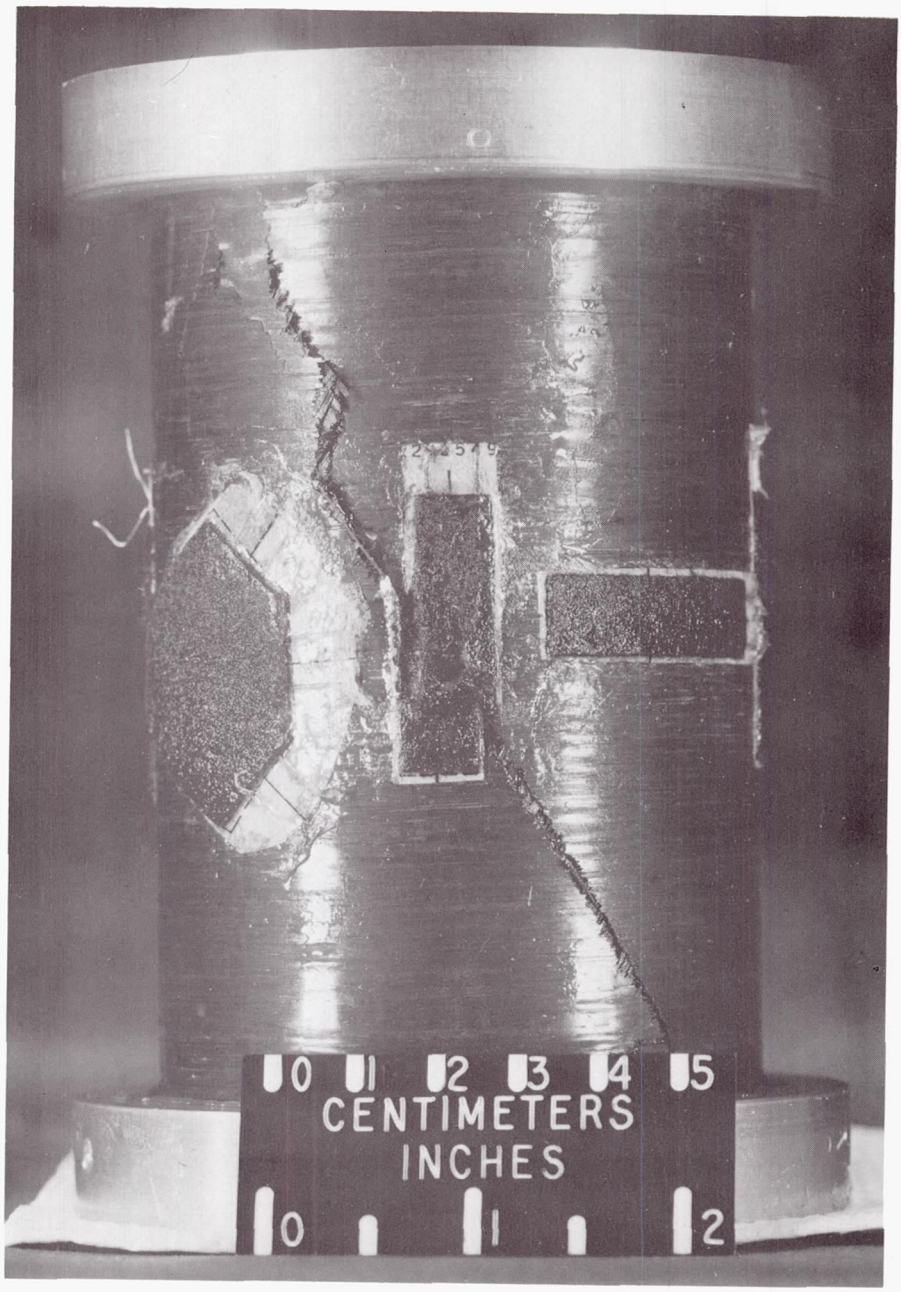

Figure 22.- Isotropic boron-epoxy cylinder failed by internal pressurization. L-66-10070

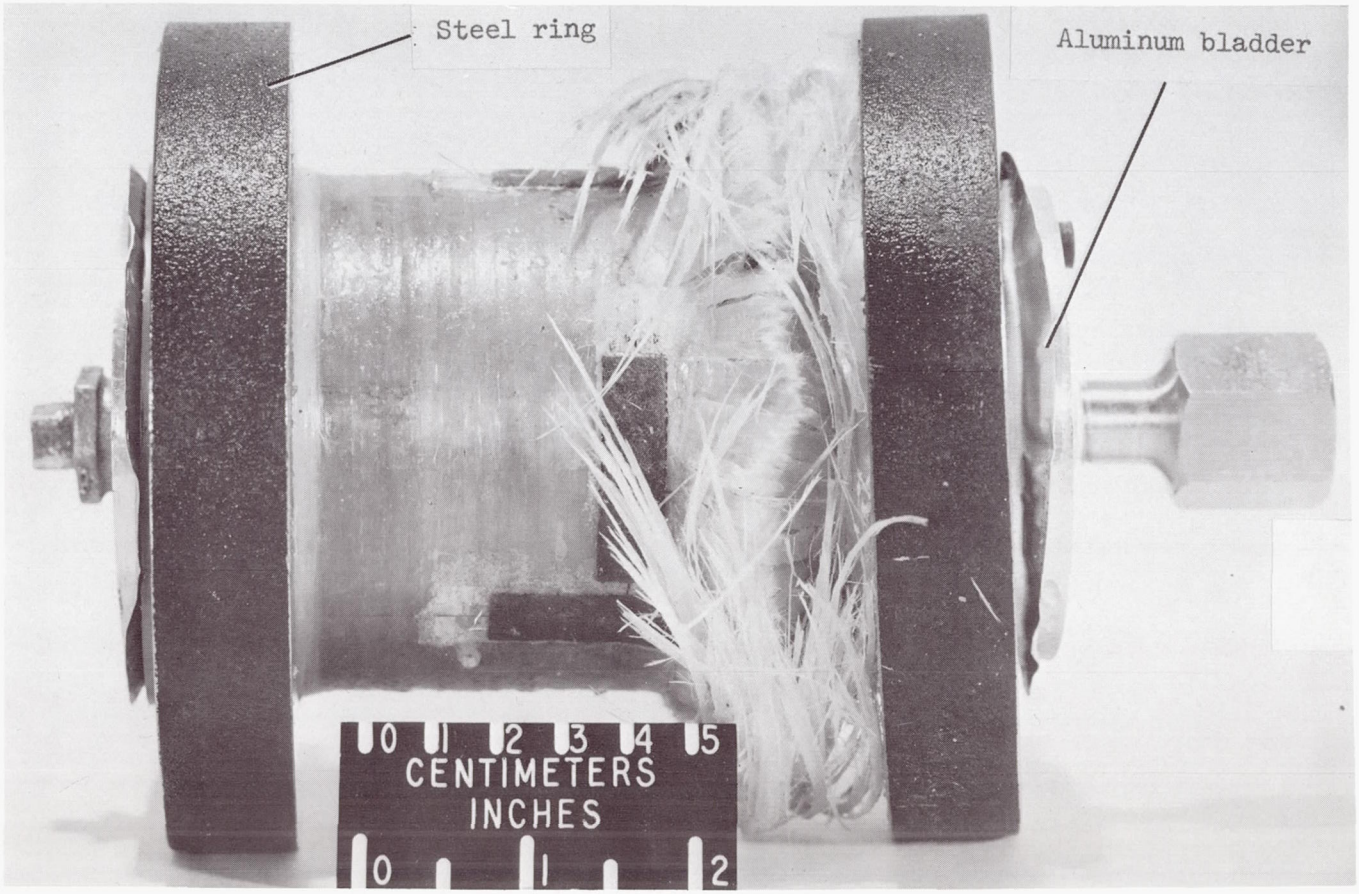

Figure 23.- Orthotropic glass-epoxy cylinder failed by internal pressurization. L-67-3882

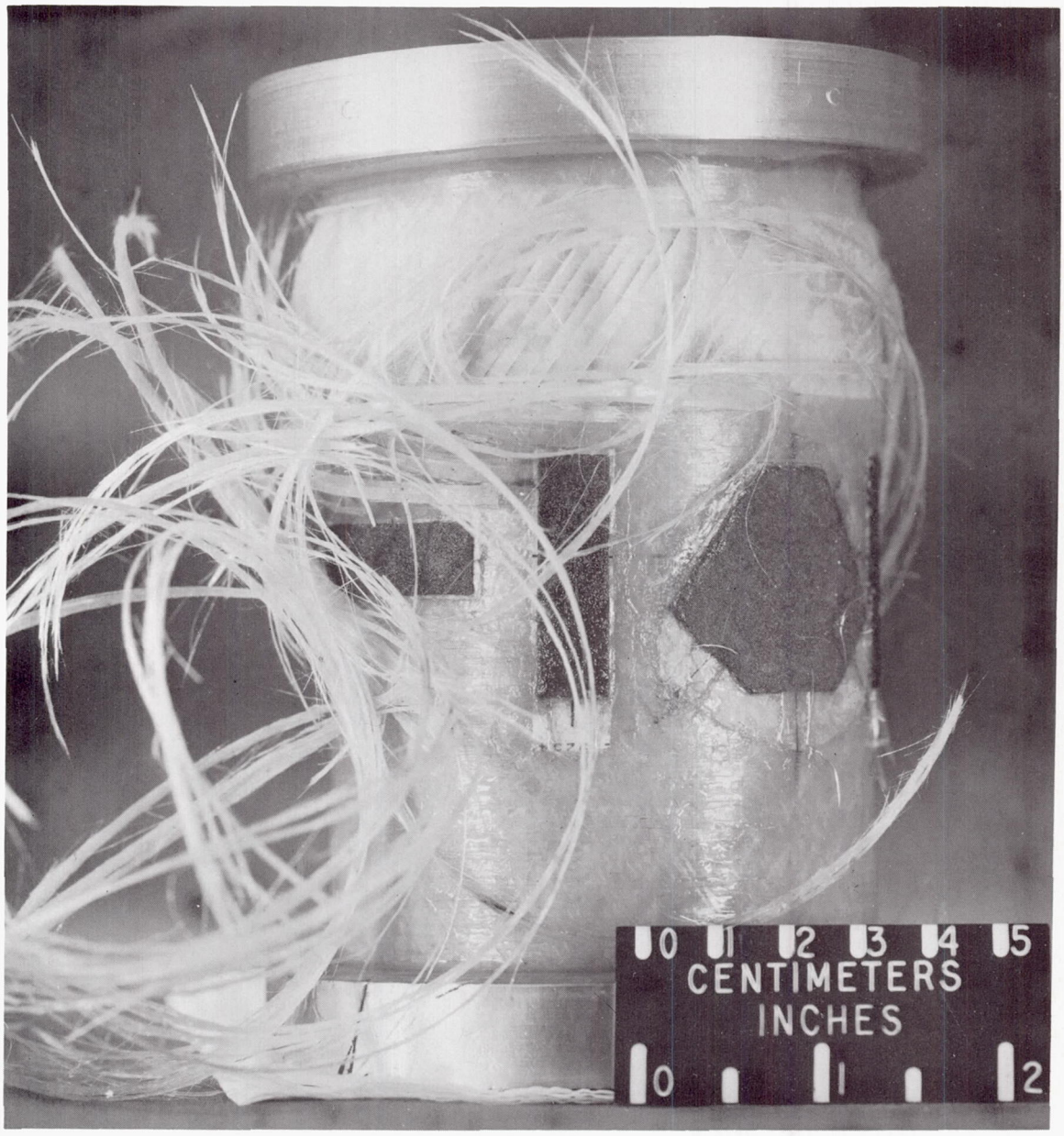

L-66-10069

Figure 24.- Isotropic glass-epoxy cylinder failed by internal pressurization.

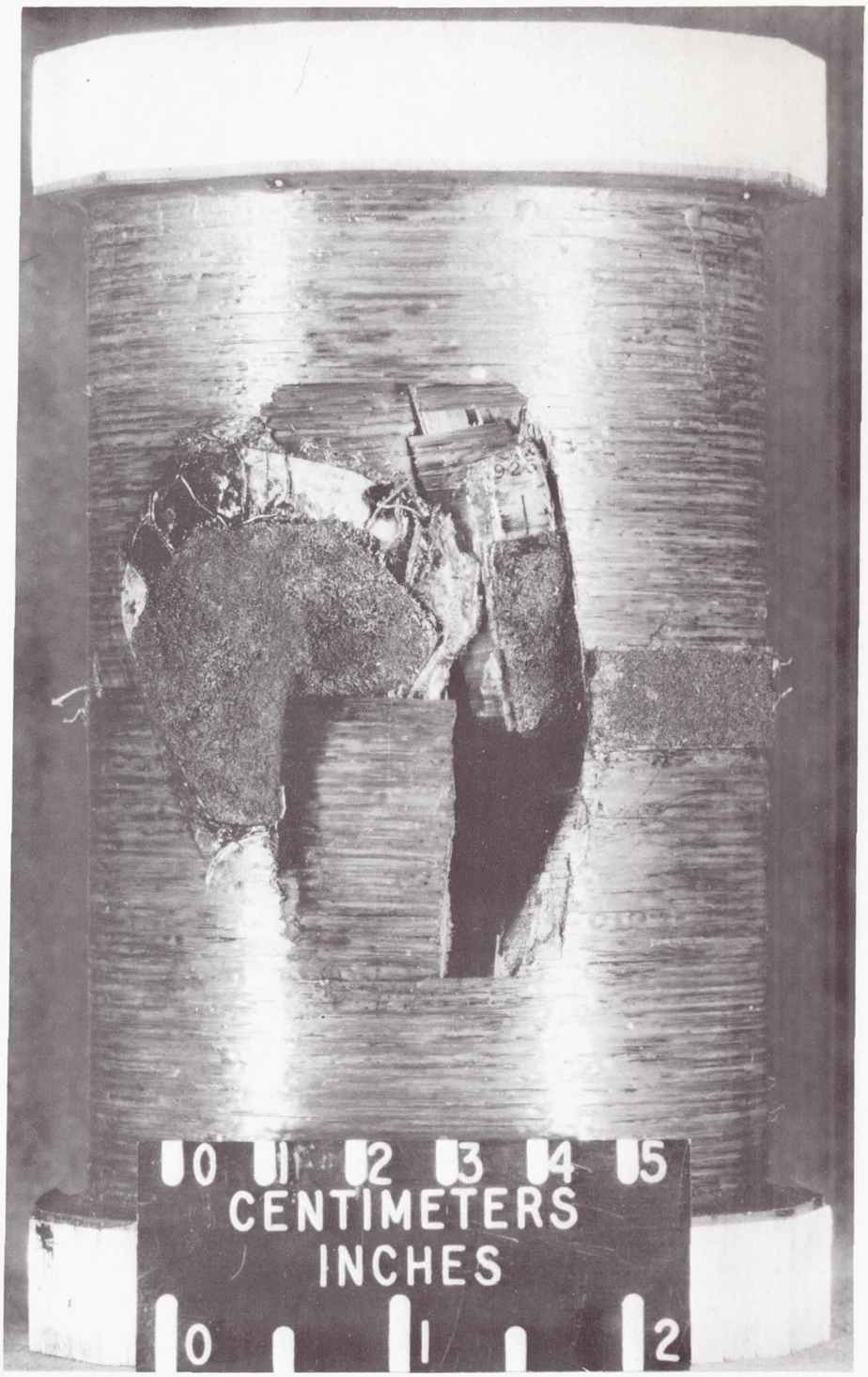

Figure 25.- Orthotropic boron-epoxy cylinder failed by external pressurization. L-67-1518

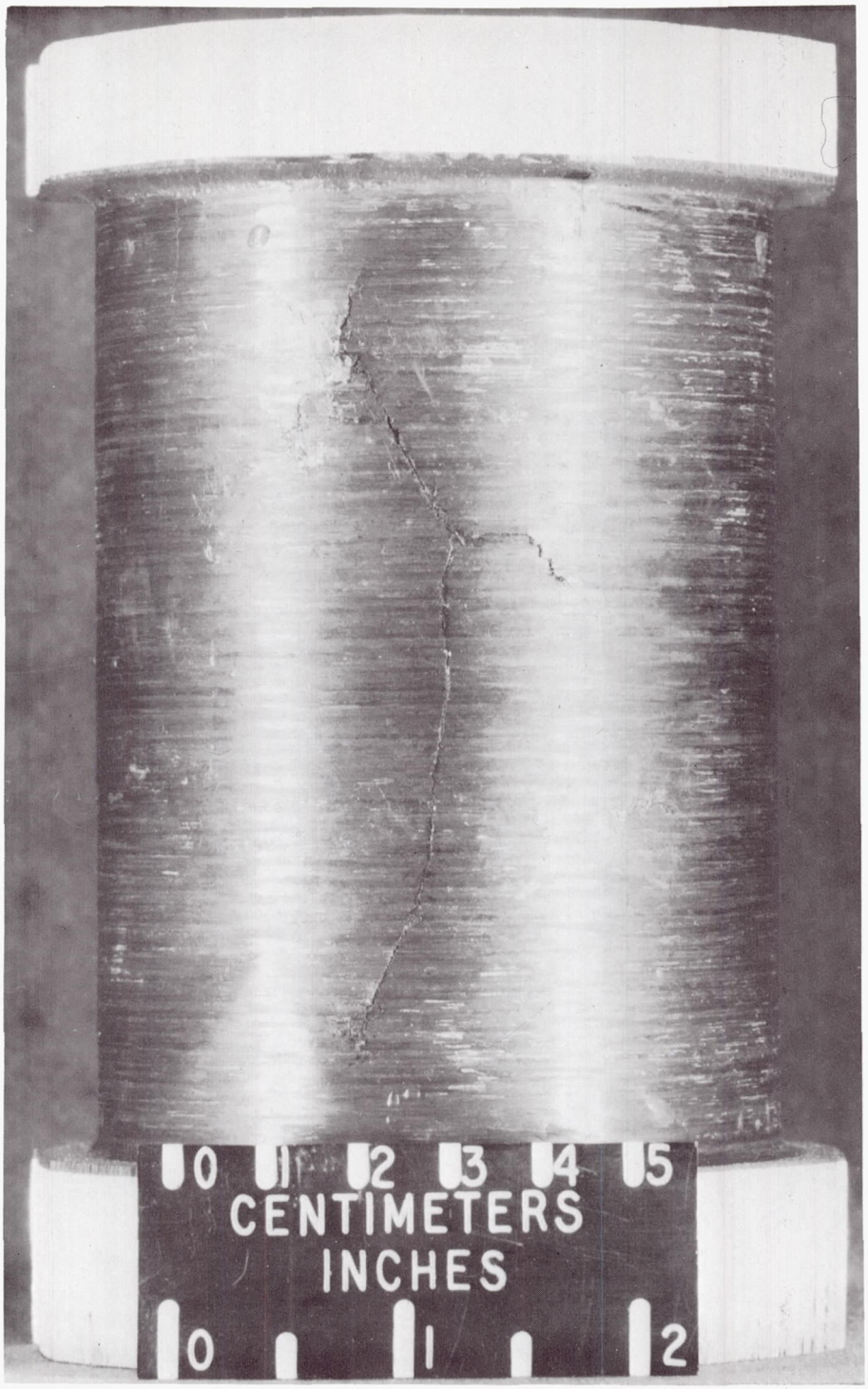

Figure 26.- Isotropic boron-epoxy cylinder failed by external pressurization. L-67-1520

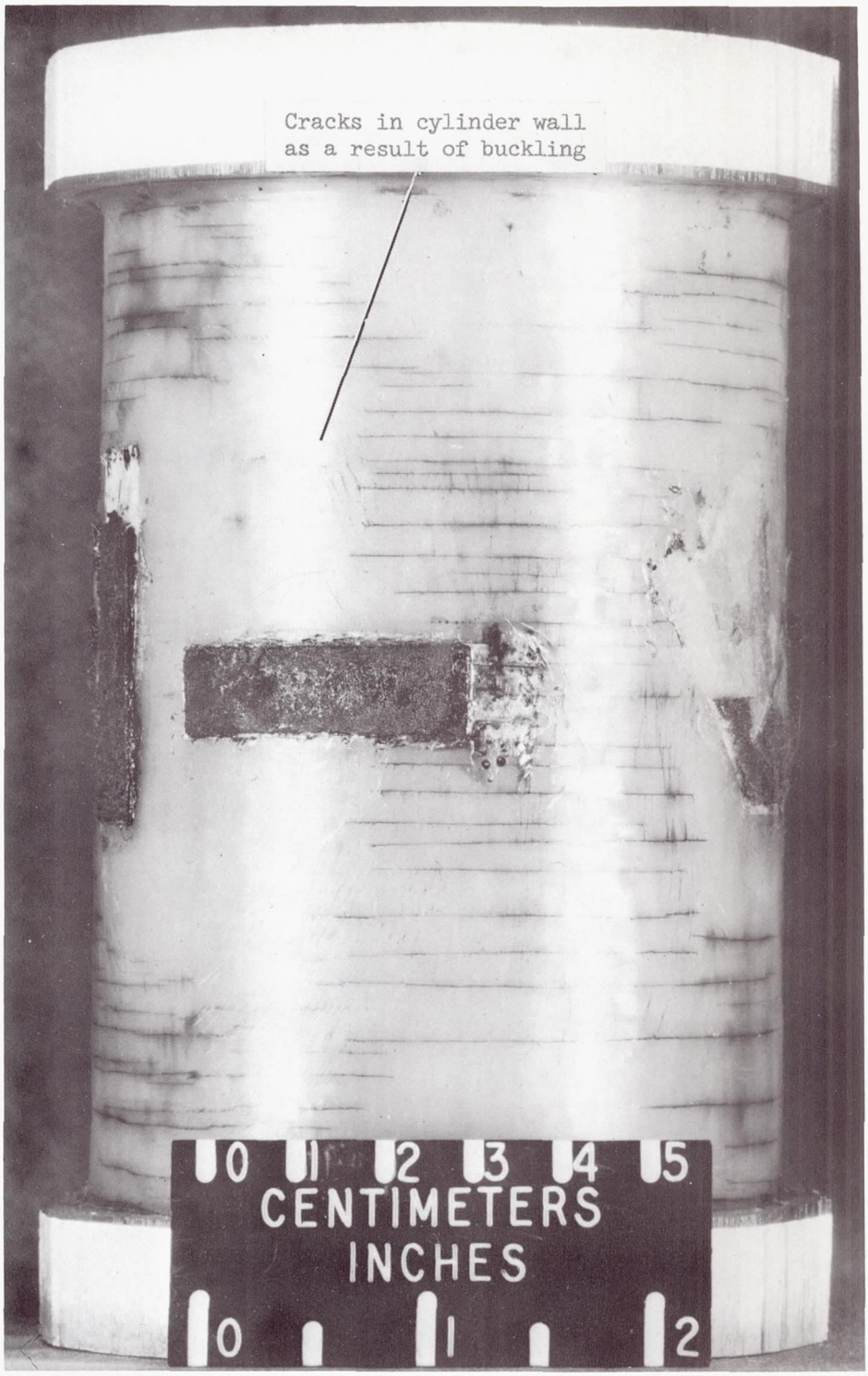

Figure 27.- Orthotropic glass-epoxy cylinder failed by external pressurization. L-67-1519.1

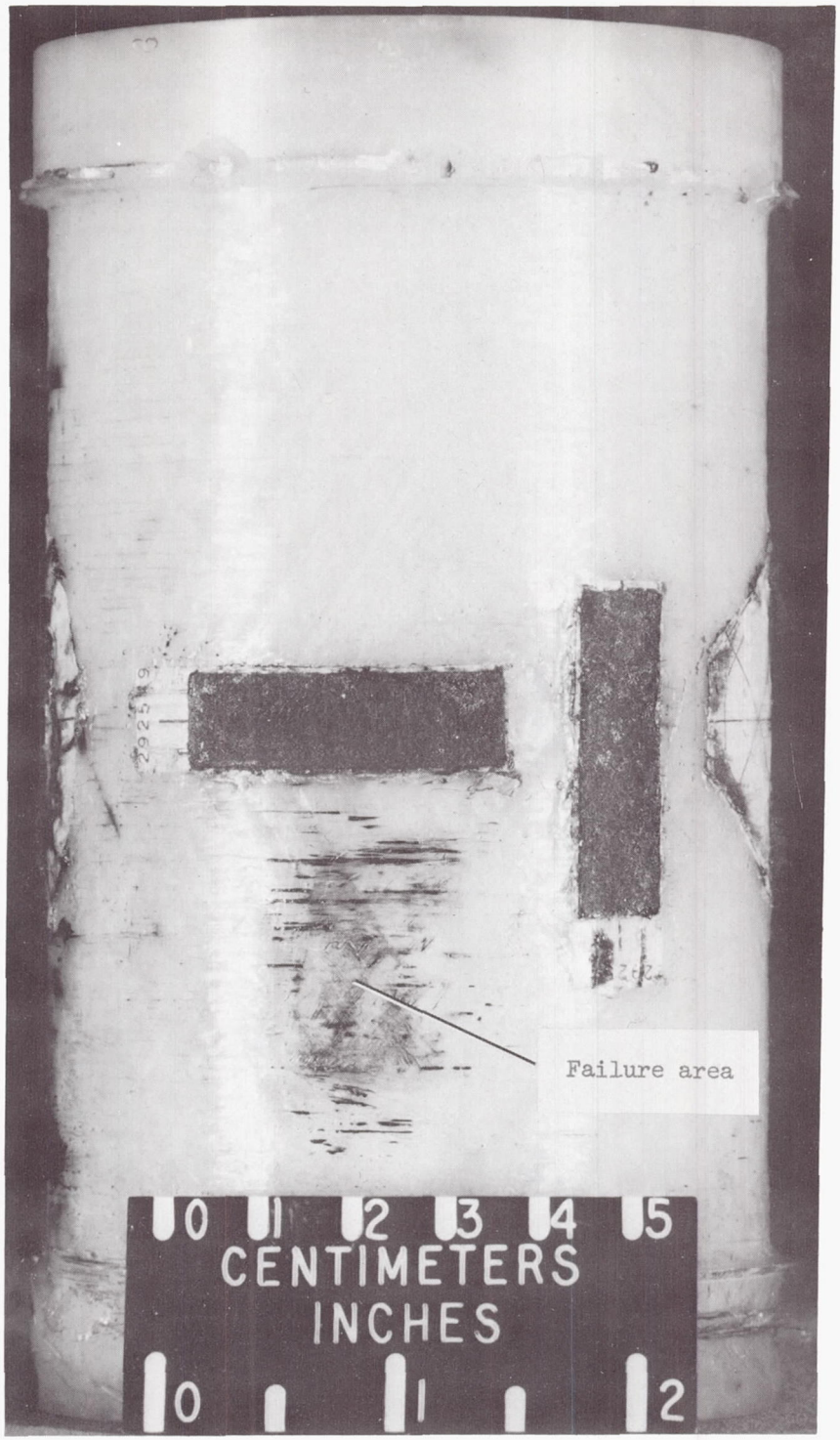

Figure 28.- Isotropic glass-epoxy cylinder failed by external pressurization. L-67-1521.1

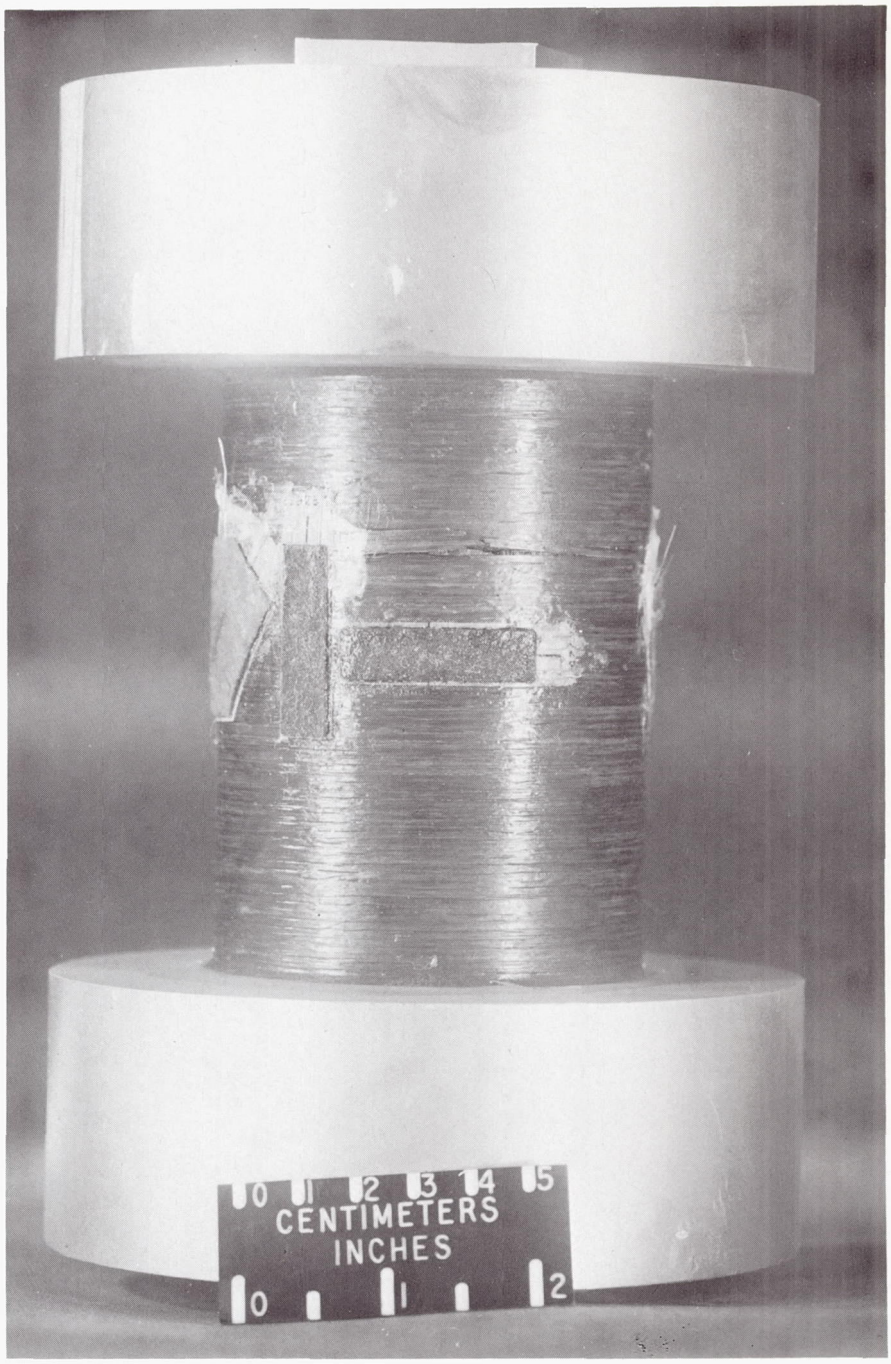

Figure 29.- Orthotropic boron-epoxy cylinder failed by axial compression. L-66-10068

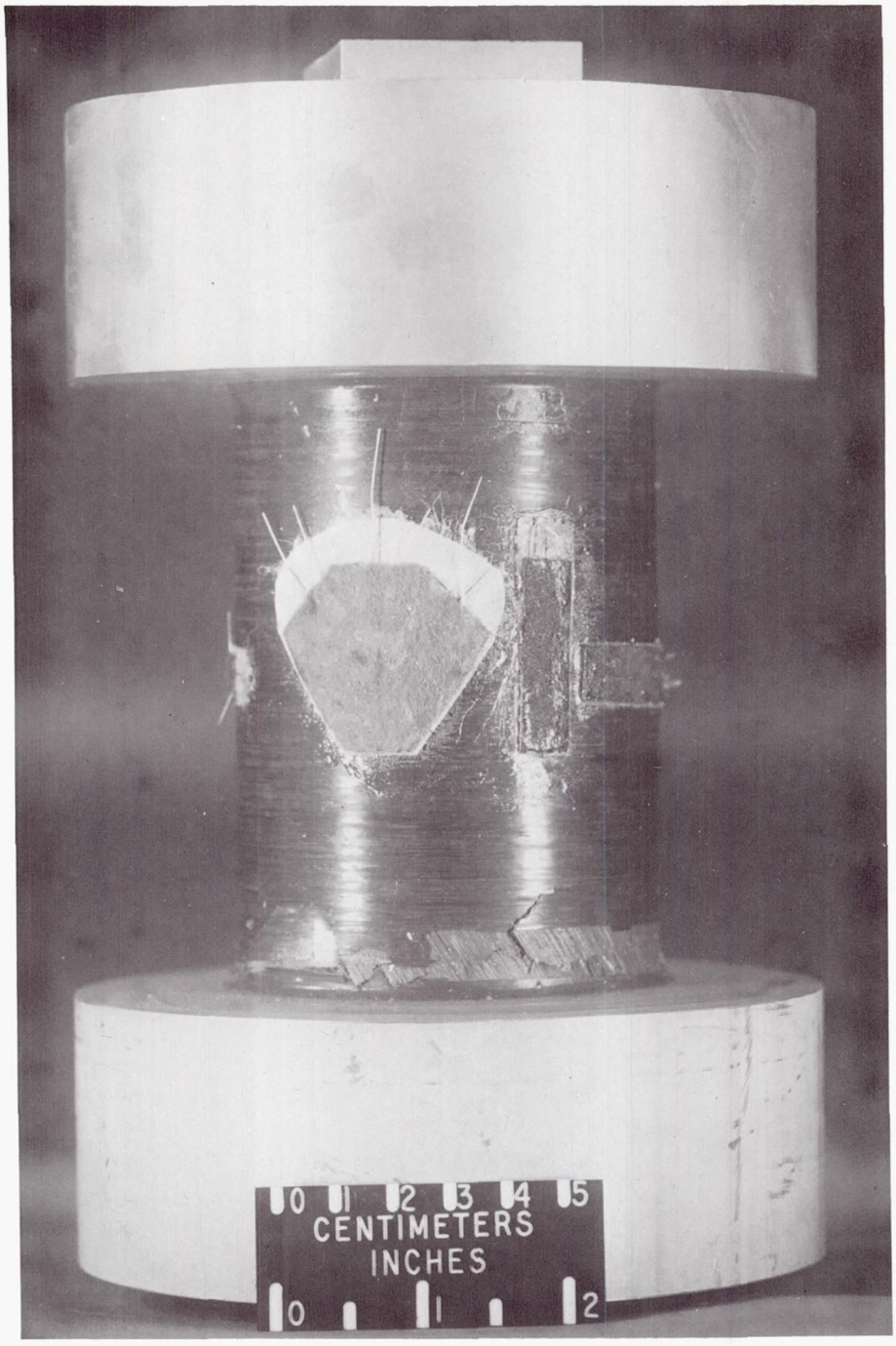

Figure 30.- Isotropic boron-epoxy cylinder failed by axial compression. L-66-10066

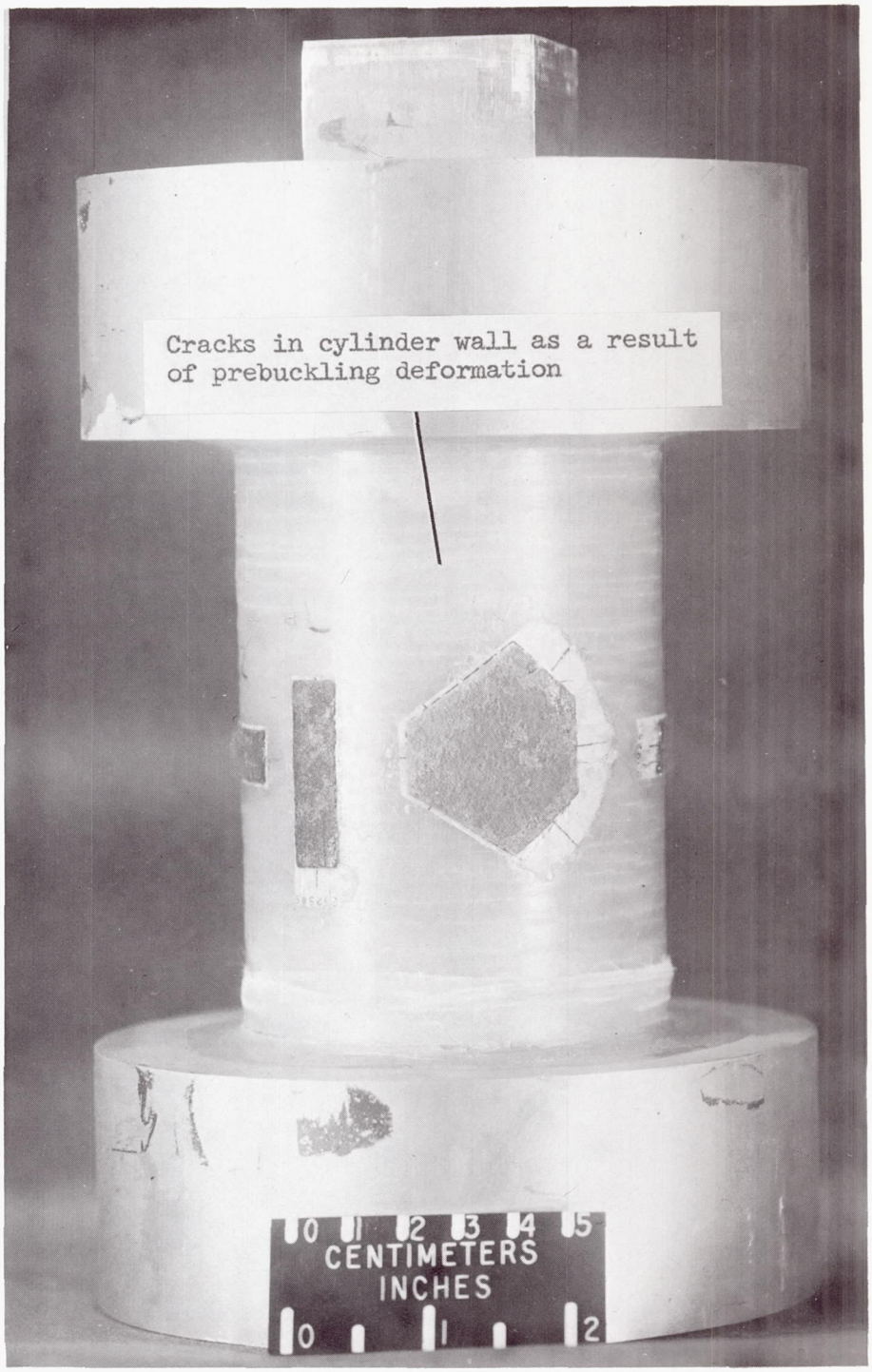

Figure 31.- Orthotropic glass-epoxy cylinder failed by axial compression. L-66-10067.1

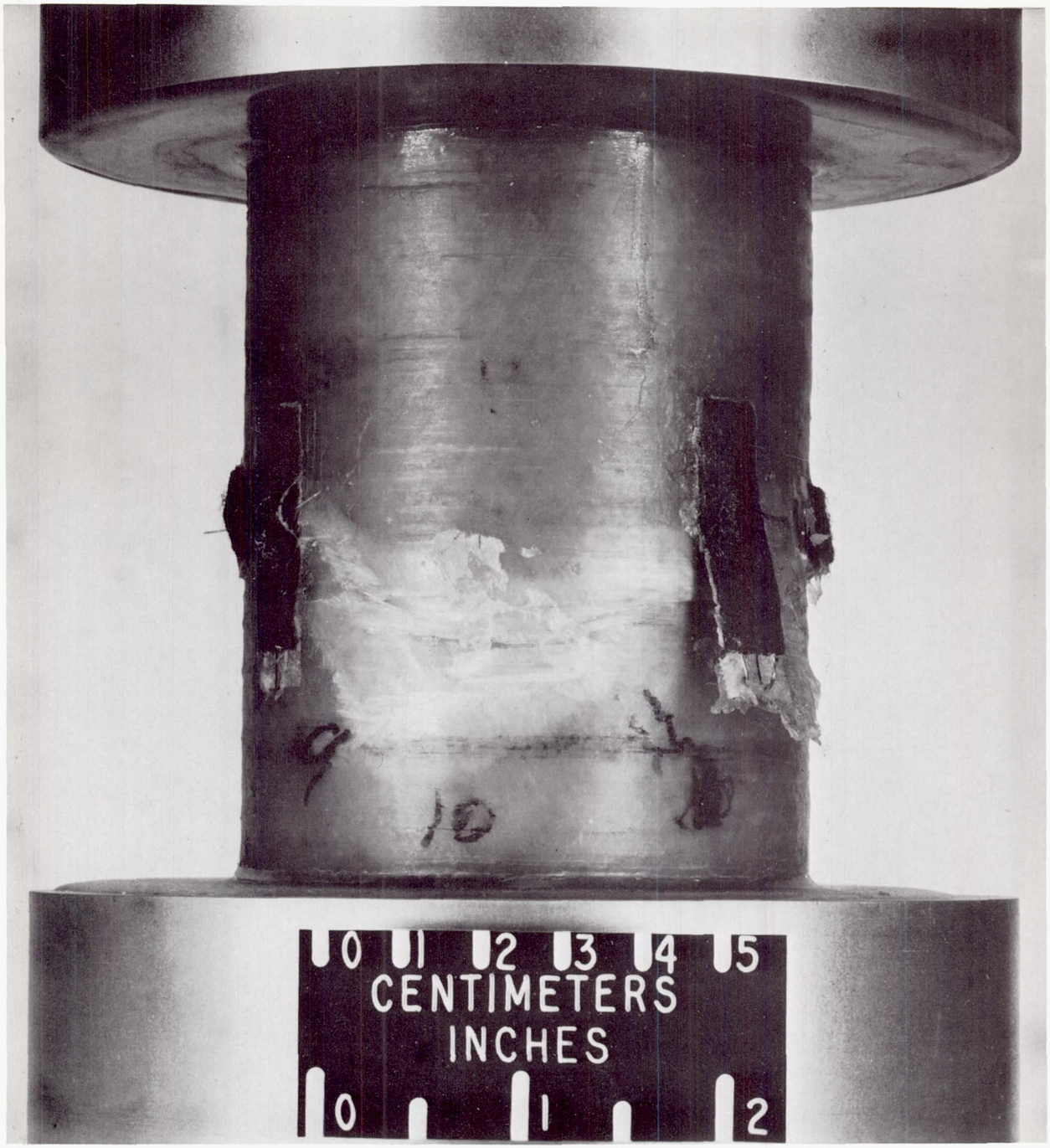

Figure 32.- Isotropic glass-epoxy cylinder failed by axial compression.

L-67-2998

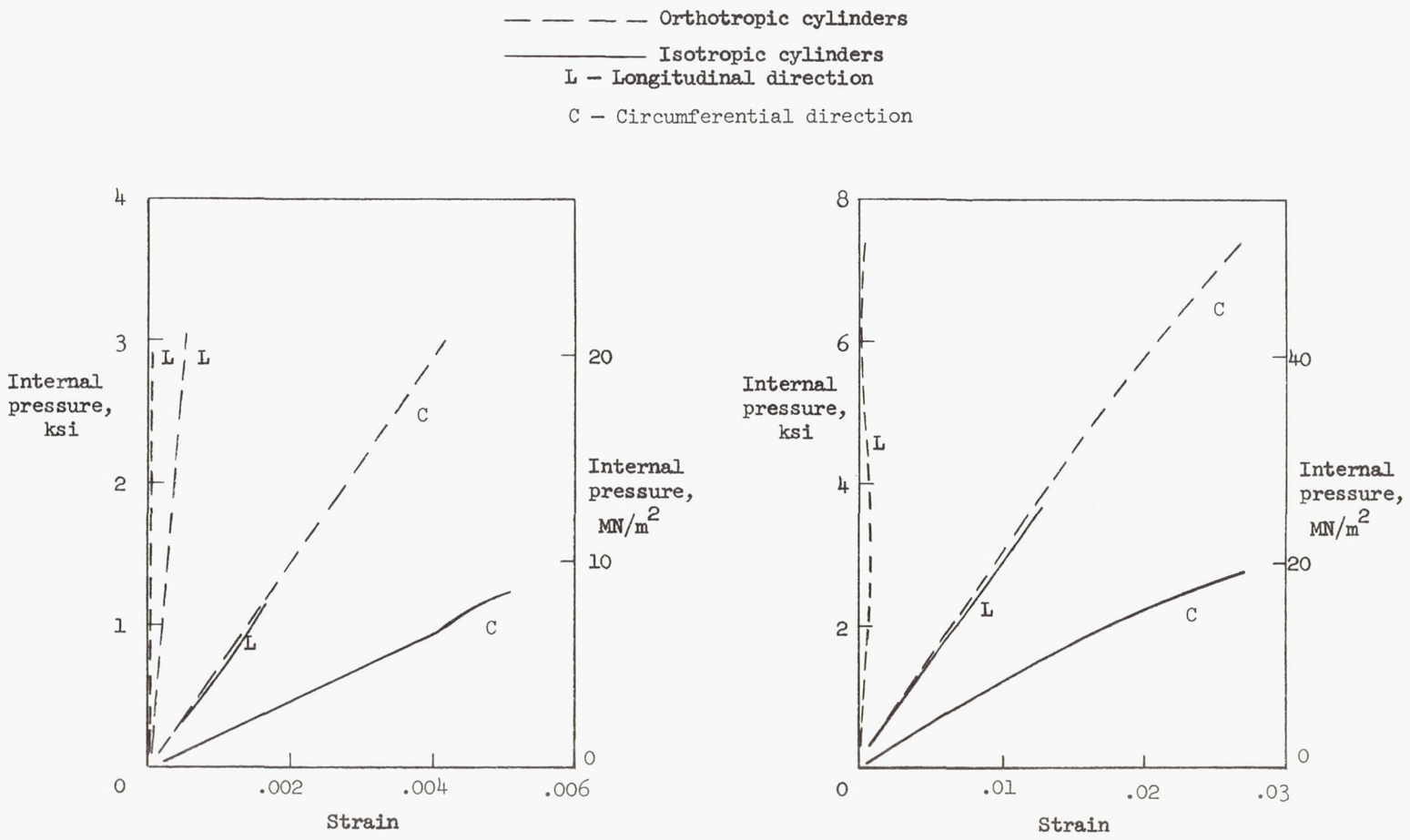

Figure 33.- Load-strain curves for internal pressure failure of boron-epoxy cylinders.

Figure 34.- Load-strain curves for internal pressure failure of glass-epoxy cylinders.

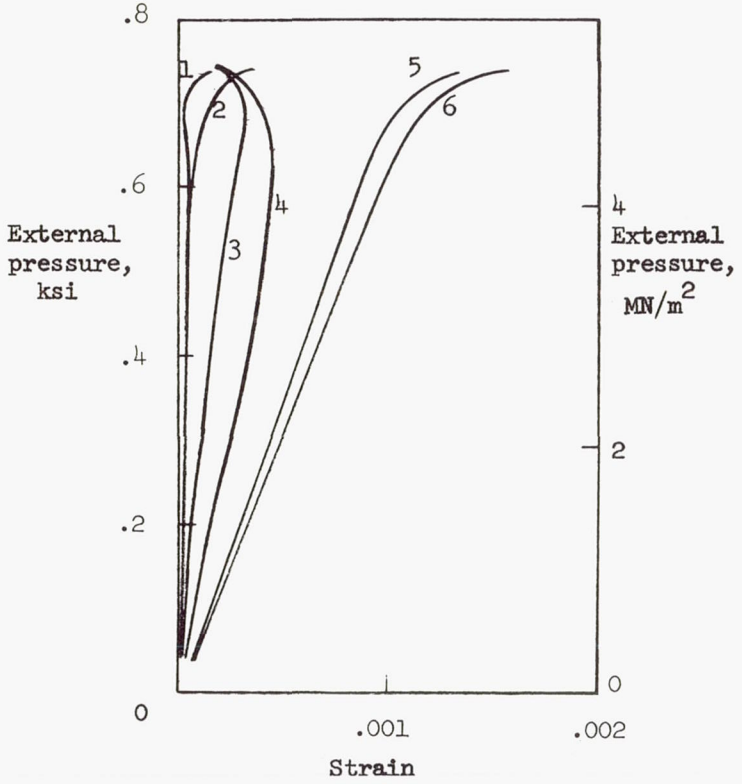

Figure 35.- Load-strain curves for external pressure failure of orthotropic boron-epoxy cylinder. Longitudinal gages are 1, 2, 3; circumferential gages are 4, 5, 6.

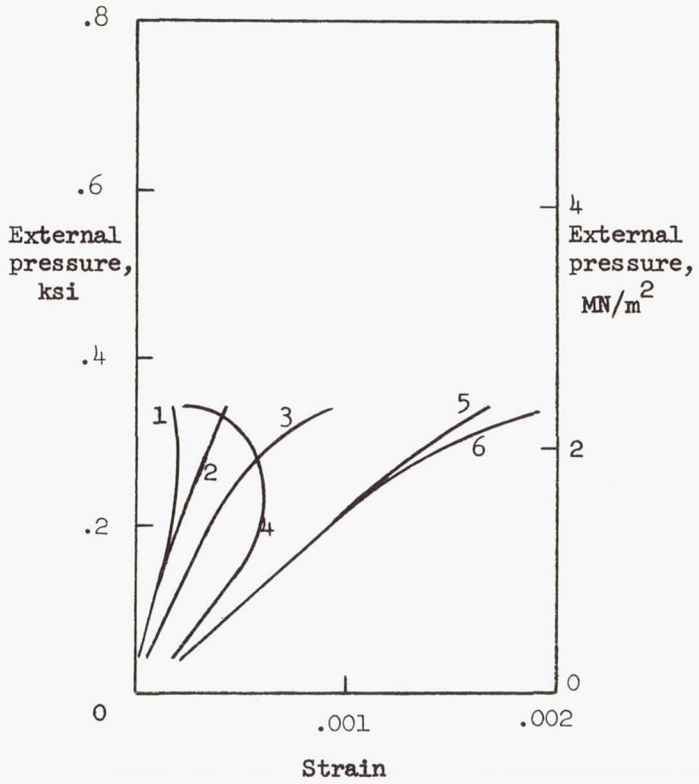

Figure 36.- Load-strain curves for external pressure failure of isotropic boron-epoxy cylinder. Longitudinal gages are 1, 2, 3; circumferential gages are 4, 5, 6.

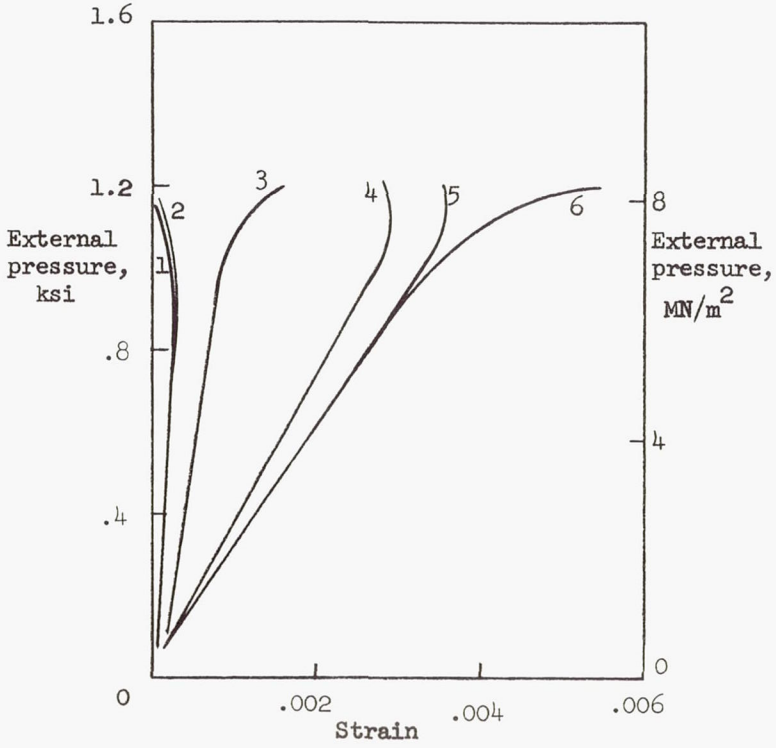

Figure 37.- Load-strain curves for external pressure failure of orthotropic glass-epoxy cylinders. Longitudinal gages are 1, 2, 3; circumferential gages are 4, 5, 6.

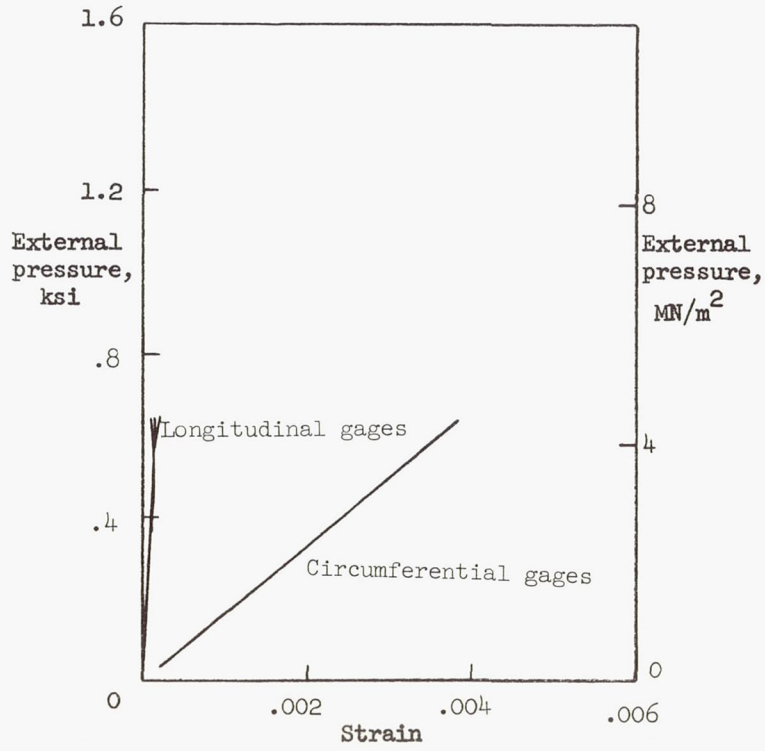

Figure 38.- Load-strain curves for external pressure failure of isotropic glass-epoxy cylinders.

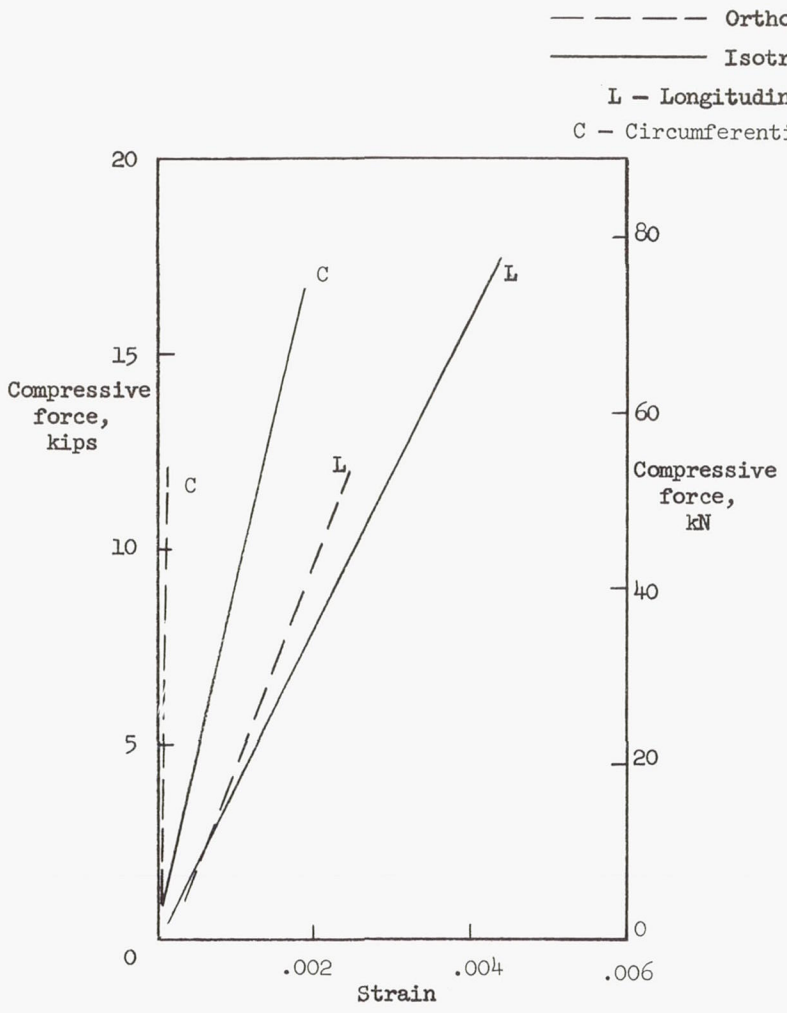

Figure 39.- Load-strain curves for axial compression failure of boron-epoxy cylinders.

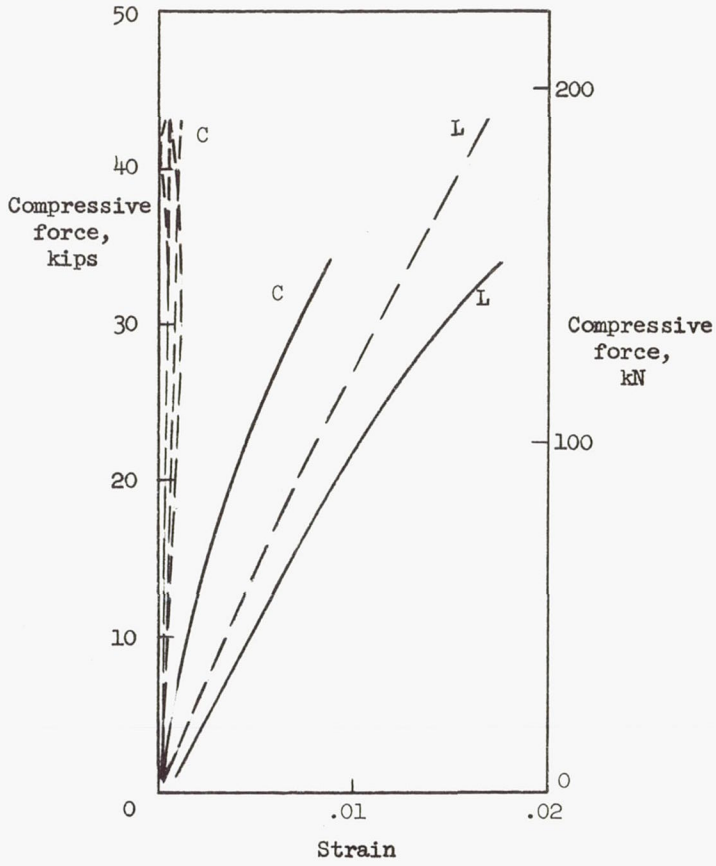

Figure 40.- Load-strain curves for axial compression failure of glass-epoxy cylinders.

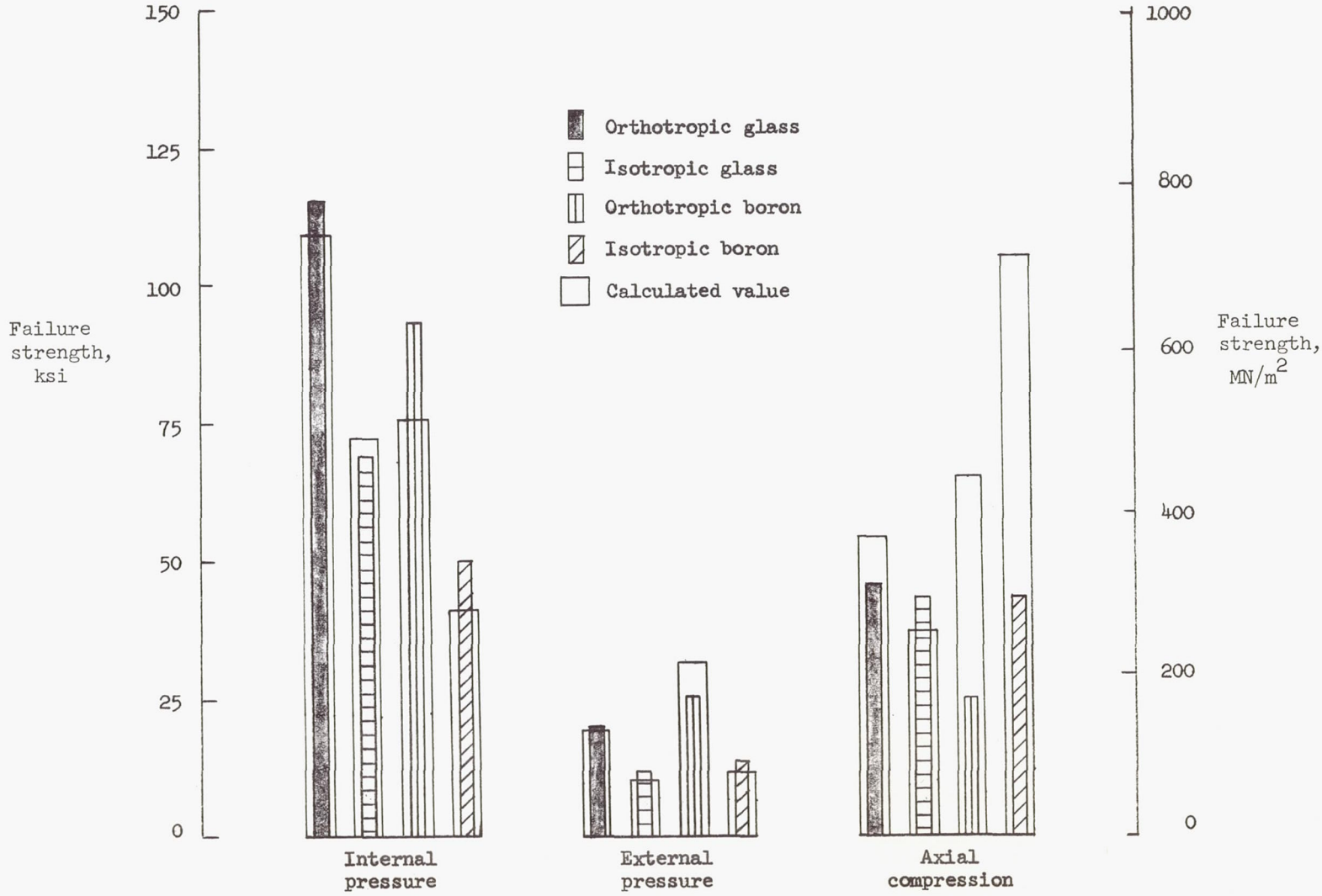

Figure 41.- Comparison of experimental and theoretically predicted failure strengths of boron-epoxy and glass-epoxy filament-wound cylinders.